NEUROSCIENCE

27-Hydroxycholesterol acts on estrogen receptor α expressed by POMC neurons in the arcuate nucleus to modulate feeding behavior

Hui Ye[1,2]†*, Xiaohua Yang[2,3]†, Bing Feng[4], Pei Luo[2,3], Valeria C. Torres Irizarry[2,5], Leslie Carrillo-Sáenz[2,5], Meng Yu[6], Yongjie Yang[6], Benjamin P. Eappen[6], Marcos David Munoz[2], Nirali Patel[2], Sarah Schaul[2], Lucas Ibrahimi[2], Penghua Lai[2]‡, Xinyue Qi[1], Yuliang Zhou[1], Maya Kota[2], Devin Dixit[2], Madeline Mun[2], Chong Wee Liew[2,5], Yuwei Jiang[2,5], Chunmei Wang[6]*, Yanlin He[4]*, Pingwen Xu[2,5]*

Oxysterols are metabolites of cholesterol that regulate cholesterol homeostasis. Among these, the most abundant oxysterol is 27-hydroxycholesterol (27HC), which can cross the blood-brain barrier. Because 27HC functions as an endogenous selective estrogen receptor modulator, we hypothesize that 27HC binds to the estrogen receptor α (ERα) in the brain to regulate energy balance. Supporting this view, we found that delivering 27HC to the brain reduced food intake and activated proopiomelanocortin (POMC) neurons in the arcuate nucleus of the hypothalamus ($POMC^{ARH}$) in an ERα-dependent manner. In addition, we observed that inhibiting brain ERα, deleting ERα in POMC neurons, or chemogenetic inhibition of $POMC^{ARH}$ neurons blocked the anorexigenic effects of 27HC. Mechanistically, we further revealed that 27HC stimulates $POMC^{ARH}$ neurons by inhibiting the small conductance of the calcium-activated potassium (SK) channel. Together, our findings suggest that 27HC, through its interaction with ERα and modulation of the SK channel, inhibits food intake as a negative feedback mechanism against a surge in circulating cholesterol.

INTRODUCTION

Oxysterols are side-chain metabolites oxidated from cholesterol molecules, which can be absorbed from the diet or generated endogenously by autooxidation or enzymatic mechanisms (*1*). Oxysterols were first proposed to act as the primary mediators for the feedback regulation of cholesterol biosynthesis in 1978 by Kandutsch *et al.* (*2*) in the Oxysterol Hypothesis of Cholesterol Homeostasis. However, subsequent studies have clarified that cholesterol itself plays an essential role in its own feedback regulation (*3*). Despite this, recent findings have revitalized interest in oxysterols as physiological regulators of cholesterol homeostasis (*4*).

27-Hydroxycholesterol (27HC) is the most abundant oxysterol found in human circulation. Its levels in the blood correlate well with cholesterol levels and may negatively modulate cholesterol synthesis (*3*, *5*, *6*). Endogenous 27HC is synthesized by the mitochondrial enzyme sterol 27-hydroxylase (CYP27A1) and catabolized by oxysterol 7α-hydroxylase (CYP7B1) as an intermediate in bile acid synthesis (*3*). 27HC, derived from and representing cellular cholesterol, has been shown to inhibit the master transcriptional regulator of lipid homeostasis (sterol regulatory element-binding protein 1) by binding to an endoplasmic reticulum protein (insulin-induced gene-2), which reduces lipogenesis and hepatic lipid accumulation (*7*–*9*). Consistently, 27HC has been reported to accelerate the degradation of 3-hydroxy-3-methyl-glutaryl-coenzyme A reductase (HMG-CoA reductase), blocking the conversion of HMG-CoA to mevalonate, which is the rate-limiting step of cholesterol biosynthesis (*10*–*12*). 27HC also functions as an alternative mechanism to high-density lipoprotein–dependent reverse cholesterol transport (RCT) to deliver sterols from peripheral tissues to the liver. This allows extrahepatic cholesterol to be excreted into bile and feces (*13*–*16*). Endogenous 27HC production may represent a defense mechanism against excessive cholesterol accumulation.

In addition to being product intermediates in the synthesis of bile acids, 27HC has been found to act as both a selective estrogen receptor modulator (SERM) and an agonist of the liver X receptor (LXR) (*17*, *18*). While 27HC can act as a mixed and tissue-specific agonist or antagonist of the estrogen receptor (ER), its effects on cell metabolism and function vary across different tissues (*17*, *19*–*22*). Notably, because of the higher polarity compared to cholesterol, 27HC diffuses much better through phospholipid membranes (*23*). Unlike cholesterol, 27HC can traverse the blood-brain barrier (BBB) from both directions in humans and animals. Its level in the brain fluctuates with physiological and pathophysiological conditions (*24*–*30*), suggesting a potential role in central metabolism. Given that both LXRs and ERs are abundantly expressed in the brain and involved in the homeostatic regulation of energy and lipid metabolism (*31*–*39*), it is likely that 27HC affects biology in the brain. 27HC has been proposed to act as an indicator of plasma cholesterol levels in the brain to modulate various central functions, including cholesterol metabolism (*40*), neural senescence (*41*), neurodegeneration (*42*), inflammatory responses (*43*, *44*), and neuronal glucose uptake

[1]School of Chemistry, Chemical Engineering and Biotechnology, Nanyang Technological University, Singapore 639798, Singapore. [2]Division of Endocrinology, Department of Medicine, The University of Illinois at Chicago, Chicago, IL 60612, USA. [3]Guangdong Laboratory of Lingnan Modern Agriculture and Guangdong Province Key Laboratory of Animal Nutritional Regulation, National Engineering Research Center for Breeding Swine Industry, College of Animal Science, South China Agricultural University, 483 Wushan Road, Tianhe District, Guangzhou, Guangdong 510642, China. [4]Pennington Biomedical Research Center, Louisiana State University, Baton Rouge, LA 70808, USA. [5]Department of Physiology and Biophysics, The University of Illinois at Chicago, Chicago, IL 60612, USA. [6]Children's Nutrition Research Center, Department of Pediatrics, Baylor College of Medicine, One Baylor Plaza, Houston, TX 77030, USA.
*Corresponding author. Email: ye.hui@ntu.edu.sg (H.Y.); chunmei.wang@bcm.edu (C.W.); yanlin.he@pbrc.edu (Y.H.); pingwenx@uic.edu (P.X.)
†These authors contributed equally to this work.
‡Present address: School of Medicine, Xiamen University, Xiamen 361102, China.

(*45*). However, it is still unclear whether 27HC regulates systemic energy homeostasis through its effects on the brain and, if so, whether these effects are mediated through LXRs and/or ERs.

Here, we investigated the central effects of 27HC on food intake, energy expenditure, and whole-body substrate utilization. Using ex vivo whole-cell patch-clamp recordings in brain slices, pharmacological blockage, Cre/Loxp- and CRISPR-mediated genetic deletion mouse models, and chemogenetics, we further identified proopiomelanocortin (POMC) neurons in the arcuate nucleus of the hypothalamus ($POMC^{ARH}$) and estrogen receptor α (ERα) as the specific neural population and receptor mediating the metabolic effects of 27HC in the brain. Last, we pharmacologically manipulated the small conductance of the calcium-activated potassium (SK) current in the arcuate nucleus of the hypothalamus (ARH) or selectively knocked out SK3 (an SK channel subtype) in the POMC neurons to explore the necessity of SK current for 27HC-mediated effects on $POMC^{ARH}$ activity and food intake.

RESULTS

Both peripheral and central administrations of 27HC induce hypophagic effects in mice

To investigate the acute metabolic effects of 27HC, we first examined its potential impact on food intake using a BioDAQ system to monitor feeding behavior. All C57BL/6J wild-type (WT) mice underwent a 6-hour light fast before starting the dark cycle. Right before the dark cycle began, the mice were intraperitoneally injected with either vehicle or 27HC (20 mg/kg). Afterward, the mice were given a chow diet. This peripheral dose of 27HC was previously shown to increase circulating 27HC levels within the physiological range, but it did not affect circulating cholesterol levels (*21*, *22*, *46*). We observed that 27HC intraperitoneal injection led to a rapid reduction in food intake in both male and female WT mice (Fig. 1, A, B, F, and G), resulting in significantly less cumulative food consumption 4 hours after peripheral delivery of 27HC (Fig. 1, C and H). The anorexigenic effects of a single intraperitoneal injection lasted for 6 hours (Fig. 1, A and F). In addition, 27HC reduced mean meal size (Fig. 1, D and I) in both female

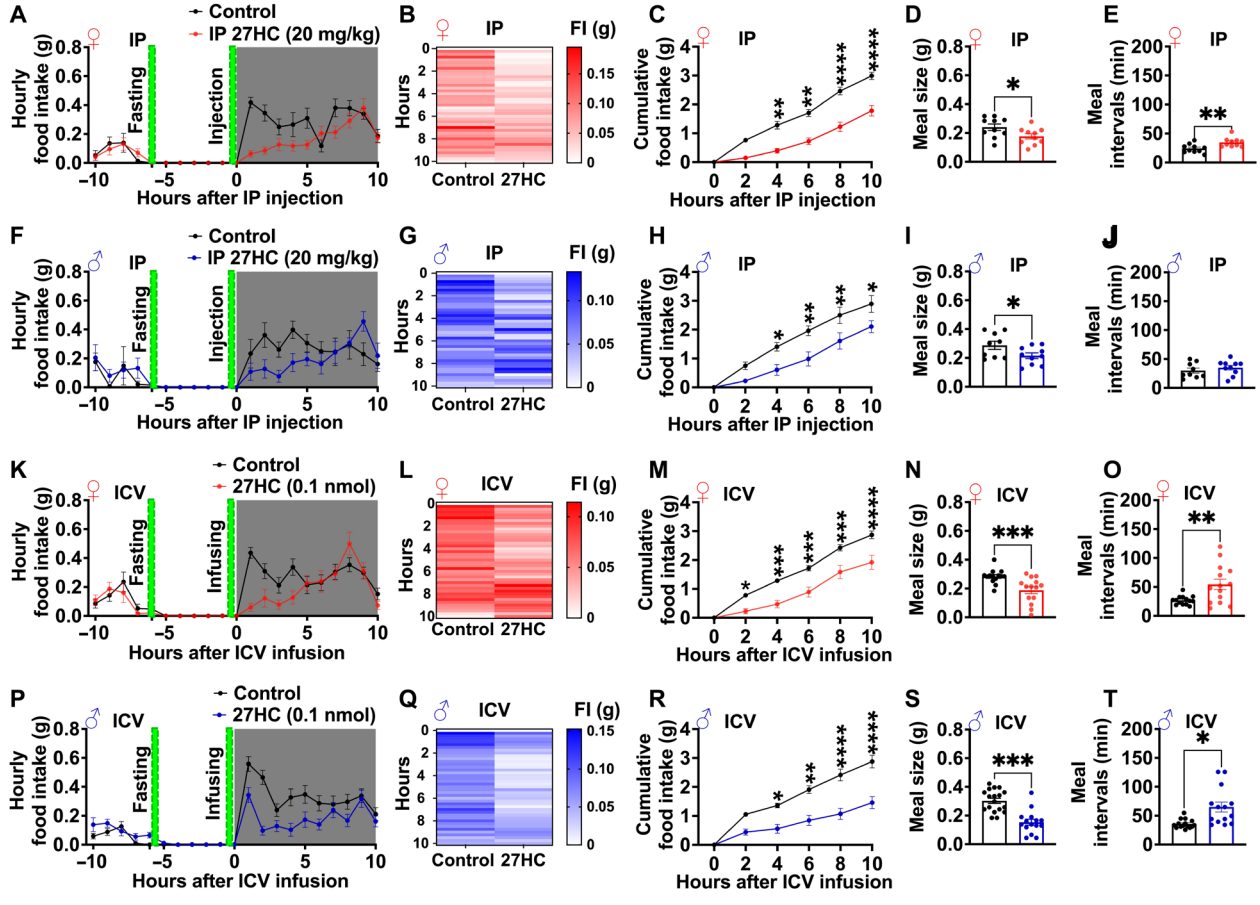

Fig. 1. 27HC acutely inhibits food intake in female and male mice. (**A** to **J**) Dark-induced food intake of 12-week-old female [(A) to (E), $n = 10$] or male [(F) to (J), $n = 10$ or 9] C57BL/6J mice after an intraperitoneal (IP) injection of 27HC (20 mg/kg) or vehicle. (**K** to **T**) Dark-induced food intake of 12-week-old female [(K) to (O), $n = 14$] or male [(P) to (T), $n = 15$] C57BL/6J mice after an intracerebroventricular (ICV) injection of 0.1 nmol 27HC or vehicle. Hourly food intake [(A), (F), (K), and (P)], a heatmap of food consumption [(B), (G), (L), and (Q), food intake recorded every 5 min], cumulative food intake [(C), (H), (M), and (R)], mean meal size [(D), (I), (N), and (S)], and mean intermeal intervals [(E), (J), (O), and (T)] 10 hours after injections. Results are shown as means ± SEM. [(C), (H), (M), and (R)] $^{*}P < 0.05$, $^{**}P < 0.01$, $^{***}P < 0.001$, and $^{****}P < 0.0001$ indicate statistical significance in a two-way analysis of variance (ANOVA) followed by post hoc Sidak tests. [(D) and (E), (I) and (J), (N) and (O), and (S) and (T)] $^{*}P < 0.05$, $^{**}P < 0.01$, and $^{***}P < 0.001$ indicate statistical significance in paired *t* tests.

and male mice. At the same time, it increased intermeal interval in females (Fig. 1E) but not males (Fig. 1J), indicating an enhancement of food intake–induced satiation and satiety.

To investigate whether the anorexigenic effects of 27HC are mediated through a central mechanism, we infused 0.1 nmol of 27HC (1 μl 100 μM) into the lateral ventricle of male and female WT mice via an intracerebroventricular cannula. The central delivery of 0.1 nmol of 27HC falls well within the daily flux of 12 μmol (5 mg) of 27HC from the circulation into the brain in humans (*24*). Consistent with the observations from the intraperitoneal injection of 27HC, we found that a single bolus intracerebroventricular infusion of 27HC quickly decreased food intake (Fig. 1, K, L, P, and Q) and resulted in a significant reduction in cumulative food consumption for both females and males (Fig. 1, M and R). We also observed that central delivery of 27HC modulated both satiation and satiety in male and female mice, as indicated by a decreased meal size and increased meal interval (Fig. 1, N, O, S, and T). Collectively, these results suggest that 27HC can modulate feeding behavior and inhibit food intake via the central nervous system.

We also observed that female mice were more sensitive to 27HC-induced anorexia compared to males. Specifically, while a low dose of 1 pmol (1 μl 1 μM) 27HC intracerebroventricular treatment had no effect on food intake or meal patterns in males, it significantly reduced food intake and meal size in female mice (fig. S1, A to J). Conversely, doses of 0.01 nmol (1 μl 10 μM) and 0.1 nmol (1 μl 100 μM) significantly reduced food intake in both male and female mice (fig. S1, A to J). These results suggest a sexual difference in the feeding response induced by the 27HC treatment.

The anorexigenic effects of 27HC induce a shift in substrate utilization

To investigate other potential central metabolic effects of 27HC, we adapted another cohort of intracerebroventricularly cannulated male and female WT mice into the Promethion metabolic chambers to measure additional metabolic parameters. Consistent with our observations in the BioDAQ system, a single bolus intracerebroventricular injection of 27HC acutely inhibited food intake in both male and female mice (Fig. 2, A and I), leading to significantly reduced cumulative food consumption 4 or 6 hours after infusion in females or males, respectively (Fig. 2, B and J).

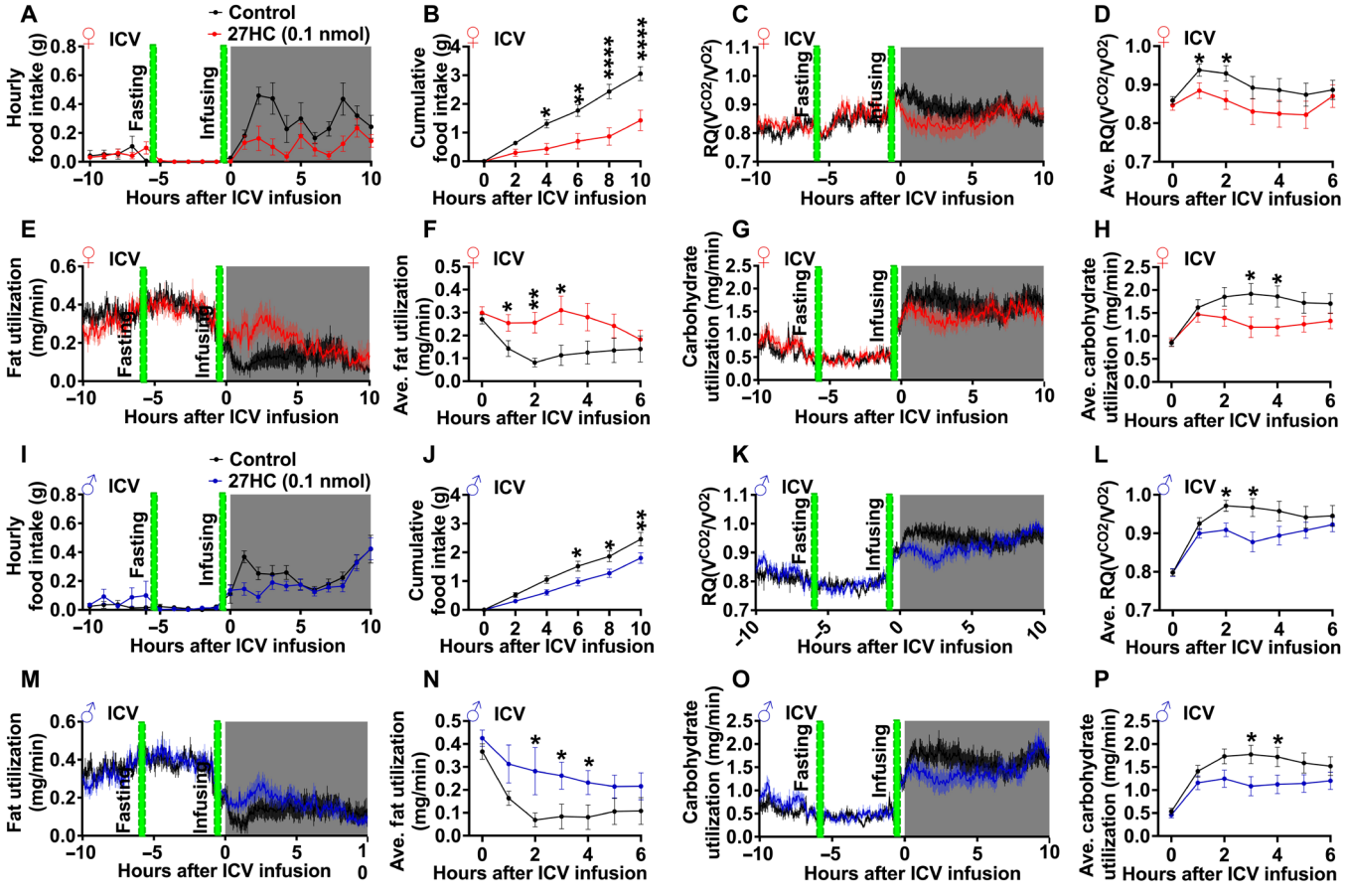

Fig. 2. A single bolus 27HC intracerebroventricular infusion induces hypophagia and alters whole-body substrate utilization in female and male mice. (**A** to **P**) Food intake and substrate utilization of 12-week-old female [(A) to (H), $n = 12$] or male [(I) to (P), $n = 14$] C57BL/6J mice after an ICV injection of 0.1 nmol 27HC or vehicle. Hourly food intake [(A) and (I)], cumulative food intake [(B) and (J)], respiratory quotient [RQ; (C) and (K)], hourly average RQ [(D) and (L)], fat utilization [(E) and (M)], hourly average of fat utilization [(F) and (N)], carbohydrate utilization [(G) and (O)], and hourly average of carbohydrate utilization [(H) and (P)] after ICV infusions. Results are shown as means ± SEM. [(B), (D), (F), (H), (J), (L), (N), and (P)] *$P < 0.05$, **$P < 0.01$, and ****$P < 0.0001$ indicate statistical significance in a two-way ANOVA followed by post hoc Sidak tests.

In line with the observed fast kinetics of feeding inhibition, we also observed a sharp decrease in the respiratory quotient (RQ; Fig. 2, C, D, K, and L), calculated as the ratio of VCO_2/VO_2, induced by 27HC intracerebroventricular injection, suggesting an acute shift in substrate utilization from carbohydrates to fat (*47*). On the basis of gaseous exchange (*48*), we further calculated whole-body fat and carbohydrate utilization. Consistent with changes in RQ, 27HC treatment led to a rapid increase in fat utilization (Fig. 2, E, F, M, and N) and a decrease in carbohydrate utilization (Fig. 2, G, H, O, and P) in both male and female mice. Notably, we did not observe statistically significant changes in VO_2 (fig. S2, A and E), VCO_2 (fig. S2, B and F), or heat production (fig. S2, C and G) in either gender. However, nonstatistical differences in VO_2 and VCO_2 could account for the changes in RQ. We also found no changes in ambulatory activity (fig. S2, D and H). Thus, these results suggest that central administration of 27HC leads to a rapid shift in whole-body substrate utilization.

This experiment was performed in the presence of food. Therefore, the effects on systemic substrate utilization could result from postprandial metabolic shifts. To explore this possibility, we investigated the regulatory effects of 27HC on substrate utilization under two scenarios: when fully fed and when fasting with no food available.

To establish a comparable satiated state between mice, we implemented an intermittent feeding paradigm in WT mice. Specifically, we restricted the daily feeding periods to 6 hours before the initiation of the dark cycle, in which the mice only ate from 12:00 p.m. to 6:00 p.m. on a 5 a.m./7 p.m. 14-hour light/10-hour dark cycle (Fig. 3A). This intermittent feeding paradigm can help reduce the stress caused by acute fasting and ensure that all mice were equally fed before the intended intracerebroventricular infusion. During the 4-day training period, we did not observe any health issues, and all the mice gradually gained weight (Fig. 3B), which is consistent with previous research (*49*). Of note, daily food intake during the 6-hour time window stabilized after 3 days of training (Fig. 3C). All mice were then adapted to the Promethion metabolic chambers and subjected to the same intermittent fasting paradigm. Following a 6-hour feeding period, food was removed from the cage, and either vehicle or 27HC was intracerebroventricularly injected. Before injection, we observed no difference in 6-hour food intake between the mice injected with vehicle or 27HC in both genders (Fig. 3, D and H), suggesting a similar level of postprandial fullness. Consistent with the findings from mice that were given food during the recording (fig. S2, A to H), we did not find statistically significant changes induced by 27HC in ambulatory activity, heat production, VO_2, and VCO_2 (fig. S3, A to H). Notably, after mice were re-fed to a similar level of postprandial fullness, the regulatory effects of 27HC on RQ and corresponding fat and carbohydrate utilization were blunted (Fig. 3, E to G and I to K).

In addition, we evaluated the effects of 27HC under fasting conditions after an 18-hour overnight fast. Consistent with the satiated state, a single bolus 27HC intracerebroventricular injection did not induce significant changes in energy expenditure, RQ, VCO_2, and VO_2 (fig. S3, I to L). Thus, these results demonstrate that the inhibitory effects of central 27HC on RQ depend on food ingestion.

27HC activates $POMC^{ARH}$ neurons in an ERα-dependent manner

On the basis of observations that central administration of 27HC induces anorexigenic effects, we postulated a central appetite-regulatory

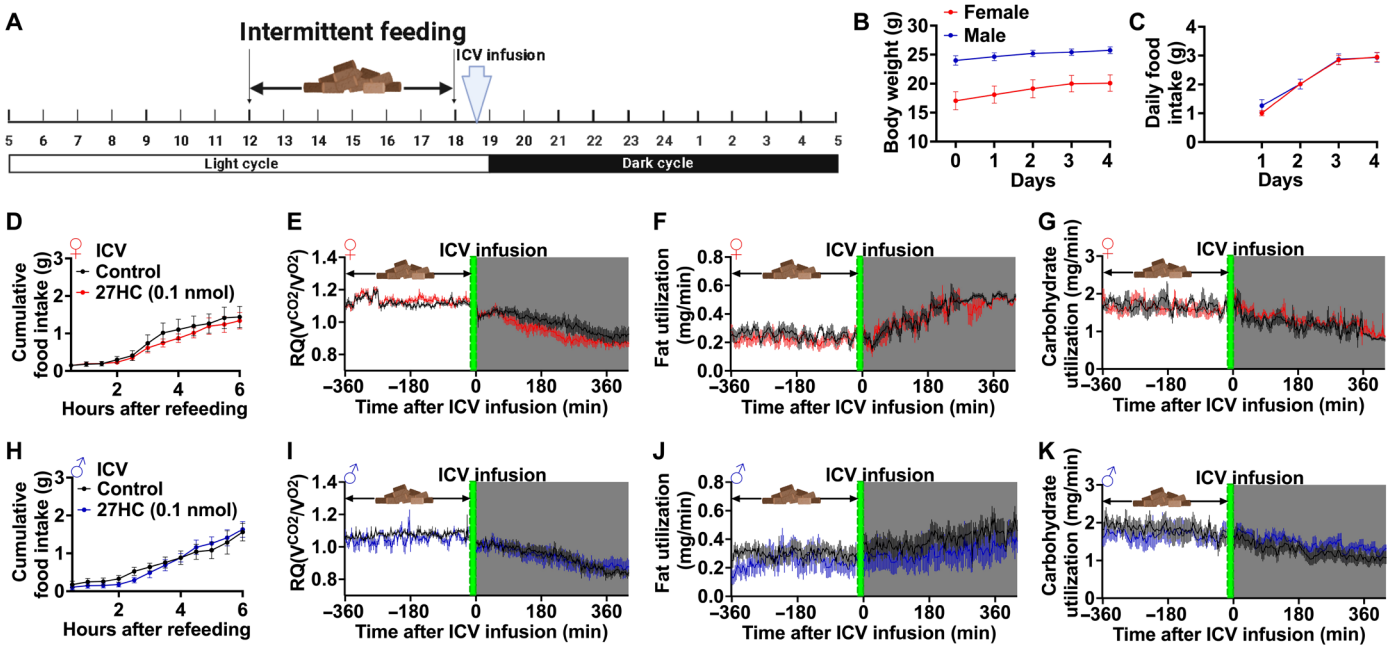

Fig. 3. A single bolus 27HC intracerebroventricular infusion does not alter whole-body substrate utilization in female and male mice in the satiated condition. (**A**) Schematic of the experimental strategy. (**B** and **C**) Body weight and daily food intake of the mice during intermittent feeding training. (**D** to **K**) Food intake before infusion and substrate utilization of 12-week-old female [(D) to (G), $n = 9$] or male [(H) to (K), $n = 8$] C57BL/6J mice after an ICV injection of 0.1 nmol 27HC or vehicle in the satiated condition. Cumulative food intake during 6-hour refeeding [(D) and (H)], RQ [(E) and (I)], fat utilization [(F) and (J)], and carbohydrate utilization [(G) and (K)] after ICV infusions. Results are shown as means ± SEM.

mechanism. Because 27HC is an endogenous SERM, and ERα in the brain modulates feeding behavior, we investigated whether 27HC regulates ERα neurons. Specifically, we performed c-Fos immunofluorescent staining in ERα-ZsGreen mice, in which ERα neurons are labeled with green fluorescence (*50*). We found that central delivery of 27HC up-regulated c-Fos expression in ERα neurons in the ARH of both male and female mice, as indicated by an increased number of ERα^{+}/c-Fos^{+} neurons (Fig. 4, A to N). Notably, there was no difference in the number of ERα^{-}/c-Fos^{+} neurons (Fig. 4, M and N), suggesting ERα-mediated stimulatory effects of 27HC on the ARH neurons. ERα is abundantly expressed in the POMC^{ARH} neurons, a well-recognized anorexigenic neuromodulator, as indicated by dual fluorescent labeling in the ARH of POMC-Cre/Rosa26-LSL-tdTOMATO/ERα-ZsGreen reporter mice (fig. S4, A to F). Previous studies suggest that female mice exhibit higher levels of ERα at the ARH (*51*). Consistent with this, we demonstrated that female mice have a higher ratio of POMC neurons colocalized with ERα in the ARH than males (fig. S4G). The ERα expressed by POMC neurons has been previously shown to mediate the estrogenic inhibition of food intake (*52*). These findings suggest that 27HC may act via ERα expressed by POMC^{ARH} neurons to inhibit feeding.

To support this model, we used whole-cell patch-clamp recordings in brain slices to examine the effects of 27HC on the neural activities of POMC^{ARH} neurons. We recorded electrophysiological responses to different doses of 27HC treatments in identified POMC^{ARH} neurons using POMC-Cre/Rosa26-LSL-tdTOMATO reporter mice (Fig. 4, O and P). We found 27HC dose-dependently depolarized POMC^{ARH} neurons with an activation rate of 43 to 55% at a dose of 100 nM or higher (Fig. 4, Q and R). To block presynaptic inputs from afferent neurons, we preincubated the brain slice with a cocktail of presynaptic blockers, including tetrodotoxin (TTX, a potent sodium channel blocker), 6-cyano-7-nitroquinoxaline-2,3-dione (CNQX, a competitive glutamate α-amino-3-hydroxy-5-methyl-4-isoxazolepropionic acid (AMPA) receptor antagonist), 2-amino-5-phosphopentanoic acid (D-AP5, a glutamate N-methyl-D-aspartate (NMDA) antagonist), and bicuculline [a competitive γ-aminobutyric acid type A ($GABA_A$) receptor antagonist]. Even in the presence of these blockers, 27HC (100 nM) still depolarized 41 to 45% of recorded POMC^{ARC} neurons (Fig. 4, S and T), suggesting a direct stimulatory effect of 27HC on POMC^{ARC} neurons. Notably, the 27HC-induced depolarization was blocked by 3,3-bis(4-hydroxyphenyl)-7-methyl-1,3,dihydro-2H-indol-2-one (BHPI, a selective ERα antagonist, Fig. 4S) but not PHTPP (a selective ERβ antagonist, Fig. 4T), indicating that ERα presumably mediates the stimulatory effects of 27HC. Therefore, our observations consistently indicate that 27HC directly activates POMC^{ARH} neurons via ERα, potentially mediating the anorexigenic effects of 27HC.

27HC is a potent agonist for LXRs, including LXRα and LXRβ. Among the LXR isoforms expressed by POMC^{ARH} neurons, LXRβ is the predominant isoform (fig. S5A) according to a secondary analysis of

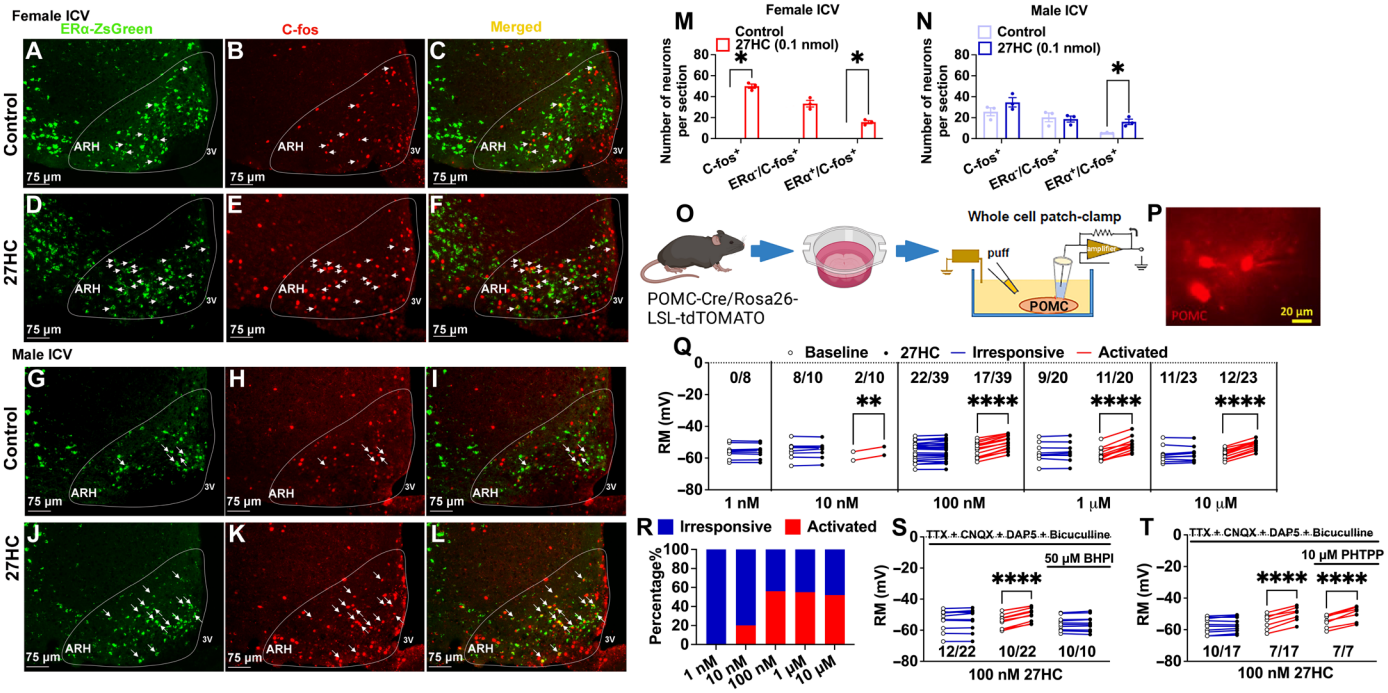

Fig. 4. 27HC activates POMC neurons via ERα. (**A** to **L**) Immunofluorescent staining for c-Fos (red) in the arcuate nucleus of the hypothalamus (ARH) of female [(A) to (F)] and male [(G) to (L)] ERα-ZsGreen mice 90 min after a single bolus ICV infusion of vehicle or 27HC (0.1 nmol). White arrows point to dual-colored neurons with ERα (green) and c-Fos (red) expressed. (**M** and **N**) Summary of quantification per section of female and male mice ($n = 3$). (**O**) Schematic of POMC neurons in the ARH (POMC^{ARH}) treated with 27HC for electrophysiology recordings. (**P**) A micrographic image showing a recorded POMC^{ARH} (red) neuron of male mice POMC-Cre/Rosa26-LSL-tdTOMATO mice. (**Q**) Resting membrane potential (RM) of POMC^{ARH} neurons before and after 27HC treatment. (**R**) Summary of the responsive ratio of POMC^{ARH} neurons for all doses of 27HC. (**S** and **T**) The effects of 100 nM 27HC on RM before and after ERα antagonist BHPI (S) or ERβ antagonist PHTPP (T) incubation. The brain slices were first preincubated with presynaptic inhibitors 1 μM TTX (a voltage-gated sodium channel blocker) + 30 μM CNQX (an AMPA receptor antagonist) + 30 μM DAP-5 (an NMDA receptor antagonist) + 50 μM bicuculline (a GABA receptor antagonist). Results are shown as means ± SEM. [(M) and (N)] $^{*}P < 0.05$ indicates statistical significance in unpaired *t* tests. [(Q), (S), and (T)] $^{**}P < 0.01$ and $^{****}P < 0.0001$ indicate statistical significance in paired *t* tests.

published RNA sequencing (RNA-seq) data (*53*). This raises the possibility that 27HC interacts with LXRβ expressed by $POMC^{ARH}$ neurons to modulate energy homeostasis. To test this possibility, we generated a mouse model with LXRβ selectively knocked down from $POMC^{ARH}$ neurons in adult mice (LXRβ-KD^{POMC}). To achieve selective knockdown, POMC-Cre mice received a bilateral stereotaxic injection of two adeno-associated virus (AAV) in the ARH (*54*, *55*). The first AAV virus expressed a small guide RNA (sgRNA) targeting the LXRβ-coding gene Nr1h2 and a Cre-dependent mCherry protein, while the second AAV carried a Cre-inducible saCas9 (fig. S5B). As a control, WT littermates received the same virus injection as experimental mice. The injection accuracy was first validated by mCherry expression selectively in the $POMC^{ARH}$ neurons (fig. S5C). LXRβ was successfully deleted with the expression of both sgRNA and saCas9 only in $POMC^{ARH}$ neurons (fig. S5D). However, LXRβ-KD^{POMC} did not affect body weight, food intake, and glucose balance under either a chow or high-fat diet condition (fig. S5, E to Z), suggesting a minor role of $LXRβ^{POMC}$ in energy homeostasis. Consistent with these findings, a single bolus intracerebroventricular injection of 27HC induced similar hypophagic effects in control and LXRβ-KD^{POMC} mice (fig. S6, A to J). Therefore, these observations narrow our interest in testing whether 27HC inhibits food intake by acting through ERα expressed by $POMC^{ARH}$ neurons.

ERα expressed by POMC neurons is required for the anorexigenic effects of 27HC

To directly test whether ERα action or POMC downstream signaling is necessary for the hypophagic effects of 27HC, we coinfused 27HC with BHPI (250 nmol) or SHU 9119 (6 nmol). SHU 9119 is a potent antagonist of melanocortin-3 and -4 receptors (MC3/4-R), which mediate the hypophagic effects of α–melanocyte-stimulating hormone (α-MSH) released from POMC neurons (*56*). Consistently, a single bolus intracerebroventricular injection of 27HC alone significantly reduced food intake, associated with decreased meal size and increased meal intervals, in both male and female mice (Fig. 5, A to J). Notably, coinfusion of BHPI or SHU 9119 completely blocked these anorexigenic effects induced by 27HC, suggesting that ERα action or POMC downstream signaling plays a mediating role. Furthermore, a single bolus intracerebroventricular infusion of 250 nmol BHPI alone did not affect food intake or feeding behavior in either gender, while 6 nmol SHU 9119 alone increased cumulative food intake and reduced satiation, as indicated by larger meal size in female but not male mice (fig. S7, A to J). The different responses to low-dose MC3/4R blockage may be attributed to gender differences in pharmacokinetics or sex-specific melanocortin circuits (*57*–*59*). These pharmacological blockage experiments support our hypothesis that 27HC inhibits food intake through ERα expressed by POMC neurons.

As a second strategy to avoid potential nonspecific impacts of pharmacologic ERα inhibition, POMC-specific ERα knockout mice were generated by crossing $Esr1^{flox/flox}$ mice and POMC-Cre mice ($Esr1^{flox/flox}$/POMC-Cre, ERα-KO^{POMC}). In line with the observations from C57BL/6J WT mice, we found that a single bolus intracerebroventricular injection of 27HC reduced dark-induced food intake and modulated feeding patterns in both female and male control $Esr1^{flox/flox}$ mice (Fig. 6, A to E and K to O). Notably, a single intracerebroventricular dose of water-soluble cyclodextrin-encapsulated 17β-estradiol (E2, 5 μg) also acutely inhibited food intake, resulting in significantly decreased cumulative food consumption after 2 hours of the intracerebroventricular infusion (Fig. 6, A to E and K to O), in both male and female control mice. This is consistent with previously reported hypophagic effects mediated by central estrogenic signaling (*32*, *60*, *61*). The similar anorexigenic effects mediated by E2 and 27HC provide additional evidence to support the agonistic action of 27HC on ERα expressed by POMC neurons. Conversely, in ERα-KO^{POMC} mice, the anorexigenic effects of 27HC or E2 were abolished entirely, as indicated by unchanged hourly food intake, cumulative food intake, meal size, and meal intervals (Fig. 6, F to J and P to T). In addition, the 27HC-induced increase of c-Fos expression in the ARH was largely reduced by ERα-KO^{POMC} (fig. S8, A to F).

Notably, the POMC-Cre mouse line has been shown to activate recombination not only in the ARH but also in other brain regions involved in energy balance, such as the nucleus of the solitary tract (NTS), which expresses ERα and is involved in food intake regulation (*62*). To further confirm whether the ARH is the mediating brain region, we generated a separate group of female mice with ERα selectively deleted in the ARH (ERα-KO^{ARH}) by injecting AAV-CMV-Cre-GFP bilaterally into the ARH of $Esr1^{flox/flox}$ mice (fig. S9, A and B). Similar to the results obtained from pharmacological blockade experiments and ERα-KO^{POMC} mice, the inhibitory effects of 27HC on food intake, as well as its modulatory effects on meal size and meal intervals, were completely abolished in the ERα-KO^{ARH} mice (fig. S9, C to L). These findings indicate that the presence of ERα in ARH neurons is crucial for the suppressive effects of 27HC on food intake.

Inhibition of $POMC^{ARH}$ abolishes 27HC-induced hypophagia

To test whether $POMC^{ARH}$ neurons mediate the inhibitory effects of 27HC on food intake, we used Designer Receptors Exclusively Activated by Designer Drugs (DREADD) technology to specifically inhibit $POMC^{ARH}$ neurons in functional mice. Specifically, we generated $hM4Di^{POMC}$ mice by stereotaxically delivering Cre-dependent inhibitory DREADD virus (AAV-hSyn-DIO-hM4Di-mCherry) into the ARH regions of the POMC-Cre mice. POMC-Cre mice that received the AAV virus carrying Cre-dependent mCherry (AAV-hSyn-DIO-mCherry) were used as a control. The accuracy of the injection was validated by mCherry immunofluorescence in the ARH of both male and female mice (fig. S10, A and B). We found that a single bolus intracerebroventricular infusion of clozapine N-oxide (CNO) alone (1 μg) did not influence the acute food intake of female control or $hM4Di^{POMC}$ mice when compared to vehicle injection (fig. S10, C and E). However, the second daily infusion of CNO significantly increased daily food intake in female $hM4Di^{POMC}$ mice but not in control mice (fig. S10, D and F), consistent with previous observations on anorexigenic effects of $POMC^{ARH}$ neurons (*63*).

In control mice, 27HC and 27HC coinfused with CNO showed similar hypophagic effects associated with corresponding changes in meal size and meal intervals (Fig. 7, A to E and K to O), excluding the potential blockage mediated by DREADD receptor–independent CNO effects. In $hM4Di^{POMC}$ mice, the acute 27HC-induced anorexigenic effects were entirely blocked by coinfusion of CNO (Fig. 7, F to J and P to T), suggesting a mediating role of $POMC^{ARH}$ neurons. In conclusion, our results demonstrate that $POMC^{ARH}$ activation is required for the hypophagic effects of 27HC.

SK3 is required for the stimulatory effects of 27HC on $POMC^{ARH}$ neurons and subsequent hypophagic response

On the basis of previous reports that the SK3 ion channel is abundantly expressed in $POMC^{ARH}$ neurons and represents a key component of

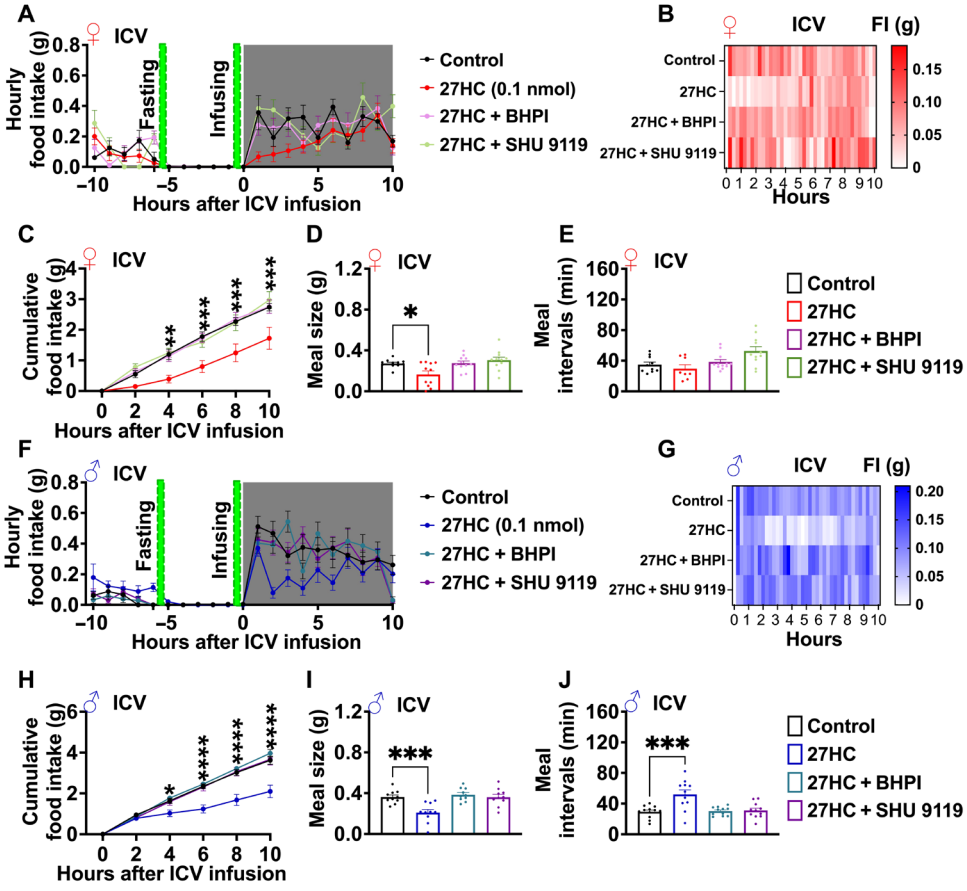

Fig. 5. ERα and melanocortin 3 and 4 receptor (MC3/4R) are required for the anorexigenic effects of 27HC in female and male mice. (**A** to **J**) Dark-induced food intake of 12-week female [(A) to (E), $n = 11$)] or male [(F) to (J), $n = 11$)] C57BL/6J mice after an ICV injection of vehicle, 0.1 nmol 27HC, 0.1 nmol 27HC + 250 nmol BHPI (27HC + BHPI), or 0.1 nmol 27HC + 6 nmol SHU9119 (27HC + SHU9119). Hourly food intake [(A) and (F)], a heatmap of food consumption [(B) and (G)], cumulative food intake [(C) and (H)], mean meal size [(D) and (I)], and mean intermeal intervals [(E) and (J)] 10 hours after injections. Results are shown as means ± SEM. [(C) and (H)] $^{*}P < 0.05$, $^{**}P < 0.01$, $^{***}P < 0.001$, and $^{****}P < 0.0001$ (27HC versus control) indicate statistical significance in a two-way ANOVA followed by post hoc Sidak tests. [(D), (E), (I), and (J)] $^{*}P < 0.05$ and $^{***}P < 0.001$ in one-way ANOVA followed by post hoc Tukey tests.

intracellular signaling integrating neuron-mediated regulatory effects on food intake and peripheral metabolic signals, including asprosin and estrogen (*55*, *64*), we examined whether SK3 is the intracellular mediator for stimulatory effects of 27HC on POMC^{ARH} neurons. We showed that a 1-s puff of 100 nM 27HC significantly reduced SK current in 44% (12 of 27) of recorded POMC^{ARH} neurons (fig. S11, A and B). This is consistent with our previous observations that estrogens act through ERα to inhibit SK current in the midbrain serotonin neurons (*65*). Given that inhibition of SK current leads to increased neuron excitability (*66*, *67*), these data support the hypothesis that 27HC inhibits SK current to activate POMC^{ARH} neurons and induce hypophagic effects.

To test this hypothesis, we implanted a guide cannula targeting the ARH of male and female WT mice. We then performed a pharmacological activation of the SK current at the ARH through an intra-ARH infusion of N-Cyclohexyl-N-[2-(3,5-dimethyl-pyrazol-1-yl)-6-methyl-4-pyrimidinamine (CyPPA), an activator of the SK current. Our results showed that ARH-specific infusion of 27HC (0.1 nmol) produced similar anorexigenic effects as intraperitoneal or intracerebroventricular injection of 27HC. However, the coinfusion of CyPPA (0.025 pmol) into the ARH completely abolished the inhibitory effects of 27HC on food intake in both genders (Fig. 8, A to J). We also found that an intra-ARH infusion of 0.025 pmol CyPPA alone did not change food intake or meal patterns (fig. S12, A to J). These results suggest that inhibition of SK current is required for the hypophagic effects mediated by 27HC ARH action.

To test the hypothesis in a genetic context, we recorded the responses of POMC^{ARH} neurons to 27HC in mice with POMC-specific deletion of the SK3 channel (SK3-KO^{POMC}, Fig. 8K), the primary subtype of SK channel expressed in POMC^{ARH} neurons (*64*, *68*, *69*). As previously reported (*64*), SK3-KO^{POMC} resulted in the depletion of SK3 protein (fig. S13, A and B), which was associated with a decrease in SK current (fig. S13C), a depolarized resting membrane potential (fig. S13D), and an increased firing frequency (fig. S13E) in POMC^{ARH} neurons. Notably, after SK3 was knocked out from POMC^{ARH} neurons, a 1-spuff of 100 nM 27HC failed to affect the SK current, resting membrane potential, and neural firing activity (Fig. 8, L to P). Consistent with these ex vivo results, SK3-KO^{POMC} also abolished the anorexigenic effects induced by ARH-specific injection of 27HC (Fig. 8, Q to Z). Together, these results support the hypothesis that the SK3 channel is required for the inhibitory effects of 27HC on the SK current and the subsequent hypophagic effects.

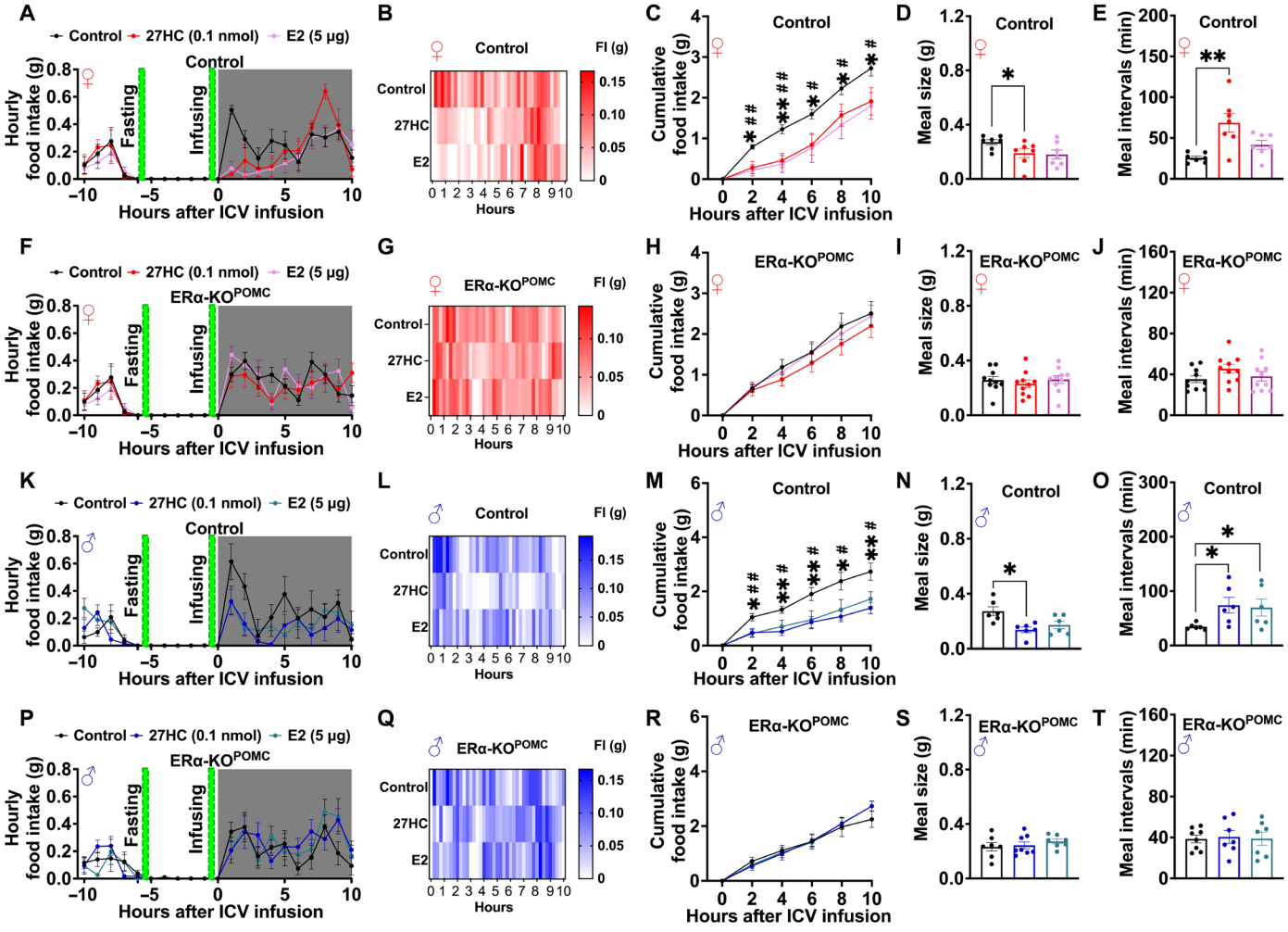

Fig. 6. ERα expressed by POMC neurons is required for the anorexigenic effects of 27HC in female and male mice. (**A** to **T**) Dark-induced food intake of 12-week female *Esr1*$^{flox/flox}$ mice [control, (A) to (E), $n = 7$], female POMC-Cre/*Esr1*$^{flox/flox}$ mice [ERα-KO^{POMC}, (F) to (J), $n = 12$], male control mice [(K) to (O), $n = 6$], or male ERα-KO^{POMC} mice [(P) to (T), $n = 8$] after an ICV injection of vehicle, 0.1 nmol 27HC, or 5 μg of cyclodextrin-encapsulated 17β-estradiol (E2). Hourly food intake [(A), (F), (K), and (P)], a heatmap of food consumption [(B), (G), (L), and (Q)], cumulative food intake [(C), (H), (M), and (R)], mean meal size [(D), (I), (N), and (S)], and mean intermeal intervals [(E), (J), (O), and (T)] 10 hours after injections. Results are shown as means ± SEM. [(C), (H), (M), and (R)] $*P < 0.05$ and $**P < 0.01$ (27HC versus control) or $\#P < 0.05$ and $\#\#P < 0.01$ (E2 versus control) indicate statistical significance in two-way ANOVA followed by post hoc Sidak tests. [(D), (E), (N), and (O)] $*P < 0.05$ and $**P < 0.01$ indicate statistical significance in one-way ANOVA followed by post hoc Tukey tests.

DISCUSSION

27HC is the most abundant oxysterol, primarily produced in the liver. It can cross the BBB and act as an indicator of plasma cholesterol levels in the brain, potentially modulating brain metabolism (*70*–*72*). The plasma levels of 27HC are highly relevant to the circulating levels of cholesterol, which fluctuate with physiological and pathophysiological conditions (*73*, *74*). Physiological levels of 27HC in the human blood range from 150 to 730 nM, with a daily flux of about 12 μmol (5 mg) 27HC from the circulation into the brain (*24*, *75*). Notably, patients with mutations in the CYP7B1, the key catabolic enzyme for 27HC, result in increased circulating levels of 27HC to 2 to 3 μM, leading to cerebrotendinous xanthomatosis characterized by adult-onset progressive neurological dysfunction (e.g., psychiatric disorders and peripheral neuropathy), or spastic paraplegia type 5, a progressive neuropathy (*76*, *77*). This suggests an essential role of 27HC in maintaining neuronal functions.

Consistent with human observations, studies in mice demonstrated a strong correlation between circulating cholesterol and 27HC levels (*73*). Physiological doses of circulating 27HC in mice range from 51.75 to 206.5 nM (20.7 to 82.6 ng/ml) (*46*, *78*) but are three to five times higher in the circulation and tissues of CYP27A1 overexpression mice (*78*). Circulating 27HC levels can increase up to threefold in pathological conditions, such as atherosclerotic lesions (*22*) or 8-week high-cholesterol/high-fat (HC/HF) diet feeding (*46*). Plasma levels of 27HC in mice are about one-third of the levels in humans (*24*, *46*, *78*), and estimating the same efficiency of BBB crossing, a daily flux of 27HC from the circulation into the brain is about 4 μmol in mice, clearly suggesting a role in brain metabolism. In supporting this view, high levels of 27HC in CYP27A1 overexpression mice impair neuronal morphology and induce synaptic dysfunction in hippocampal neurons (*79*, *80*). Increased 27HC levels induced by 11-week HFD feeding are associated with bidirectional regulation in ERα and ERβ expression and interfere

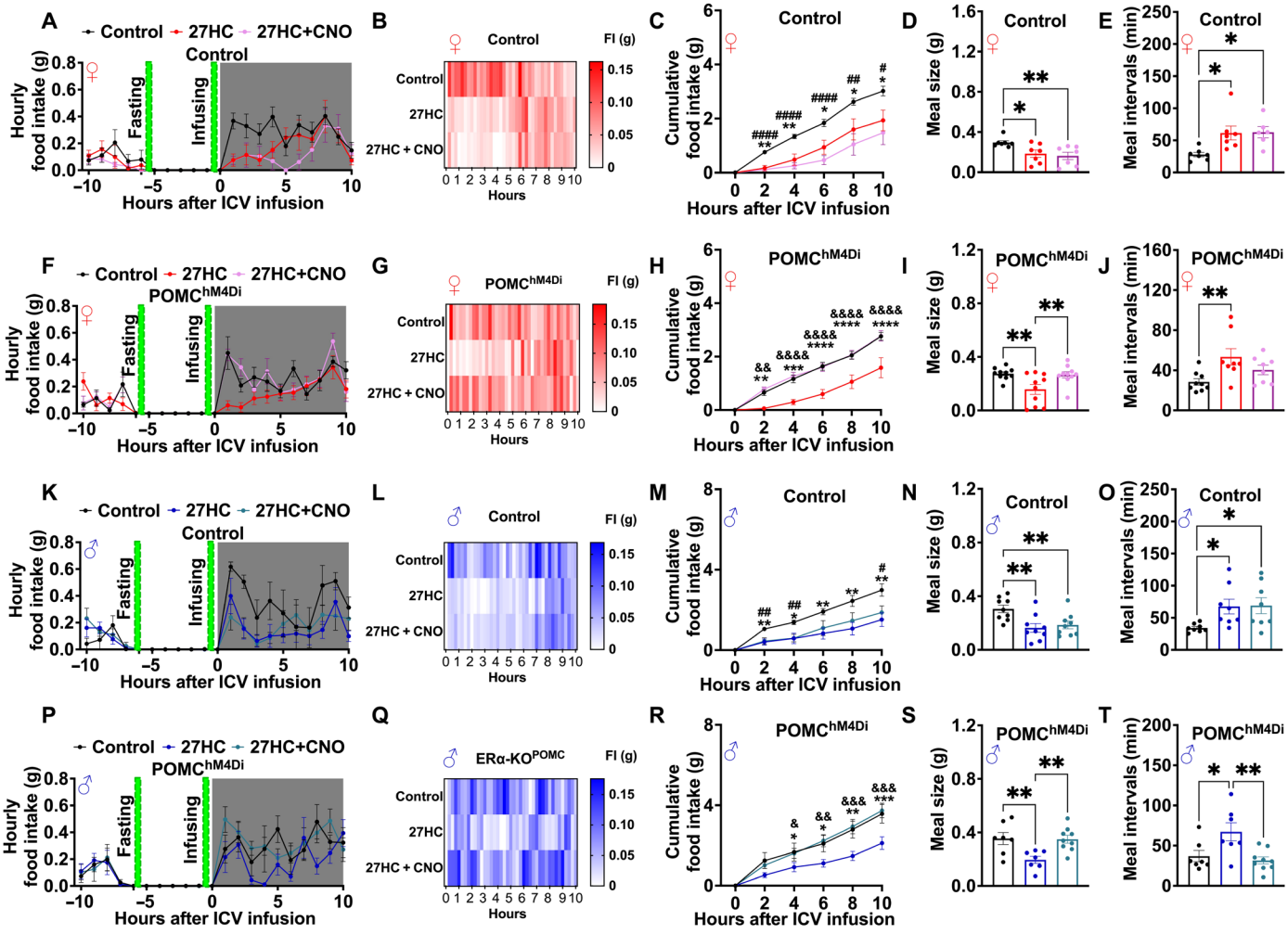

Fig. 7. Chemogenetic inhibition of POMC^{ARH} neurons abolishes the 27HC-induced hypophagia in female and male mice. (**A** to **T**) Dark-induced food intake of 12-week female POMC-Cre mice injected with AAV-EF1a-DIO-mCherry into the ARH [Control, (A) to (E), $n = 6$], female POMC-Cre mice injected with AAV-EF1a-DIO-hM4D(Gi)-mCherry [POMC^{hM4Di}, (F) to (J), $n = 10$], male Control mice [(K) to (O), $n = 9$], or male POMC^{hM4Di} mice [(P) to (T), $n = 8$] after an ICV injection of vehicle, 0.1 nmol 27HC, or 0.1 nmol 27HC + 1 μg of Clozapine N-oxide (27HC + CNO). Hourly food intake [(A), (F), (K), and (P)], a heatmap of food consumption [(B), (G), (L), and (Q)], cumulative food intake [(C), (H), (M), and R)] mean meal size [(D), (I), (N), and (S)], and mean intermeal intervals [(E), (J), (O), and (T)] 10 hours after injections. Results are shown as means ± SEM. [(C), (H), (M), and R)] *$P < 0.05$, **$P < 0.01$, ***$P < 0.001$, and ****$P < 0.0001$ (27HC versus control); #$P < 0.05$, ##$P < 0.01$, and ####$P < 0.0001$ (27HC + CNO versus control); or &$P < 0.05$, &&$P < 0.01$, &&&$P < 0.001$, and &&&&$P < 0.0001$ (27HC versus 27HC + CNO) indicate statistical significance in two-way ANOVA followed by post hoc Sidak tests. [(D), (E), (I), (J), (N), (O), (S), and (T)] *$P < 0.05$ and **$P < 0.01$ indicate statistical significance in one-way ANOVA followed by post hoc Tukey tests.

with neurodegeneration in animal models (*26*). All of these indicate the potential physiological effects of 27HC in the central nervous system.

It has been shown that brain 27HC reduces insulin-mediated glucose uptake and neuronal glucose metabolism, which may be associated with changes in central metabolism (*45*, *81*). Despite this critical evidence regarding the role of 27HC in modulating neuronal glucose uptake, the direct effects of central 27HC on whole-body energy homeostasis are still unknown. We found that a single bolus intraperitoneal, intracerebroventricular, or intra-ARH injection of 27HC can produce profound anorexigenic effects associated with a shift of substrate utilization induced by food ingestion, clearly indicating acute systemic metabolic effects of brain 27HC.

Subsequently, we conducted indirect calorimetry tests to examine the relationship between the anorexigenic effect induced by 27HC and changes in substrate utilization. These tests were performed on mice with different nutritional statuses, including satiated (fed after intermittent fasting) or overnight fasting status. When no food was provided, a single bolus 27HC intracerebroventricular injection did not significantly change the RQ, suggesting that the switch in substrate utilization depends on the reduction in food intake. However, one caveat of our studies is that RQ estimations only reflect the overall net balance of oxidized substrates and do not provide critical information on the in vivo kinetics of substrate utilization, such as the rates of production, appearance, or disappearance of metabolites. The animal body is in a constant state of turnover, with synthesis, breakdown, and conversion of compounds (*82*). The dynamic nature of in vivo kinetics of substrate metabolism can vary under different conditions, including fed conditions and stressed conditions like overnight fasting, diabetes, and obesity (*83*). Further studies using stable isotope tracers in conjunction with gas or liquid chromatography mass spectrometry and

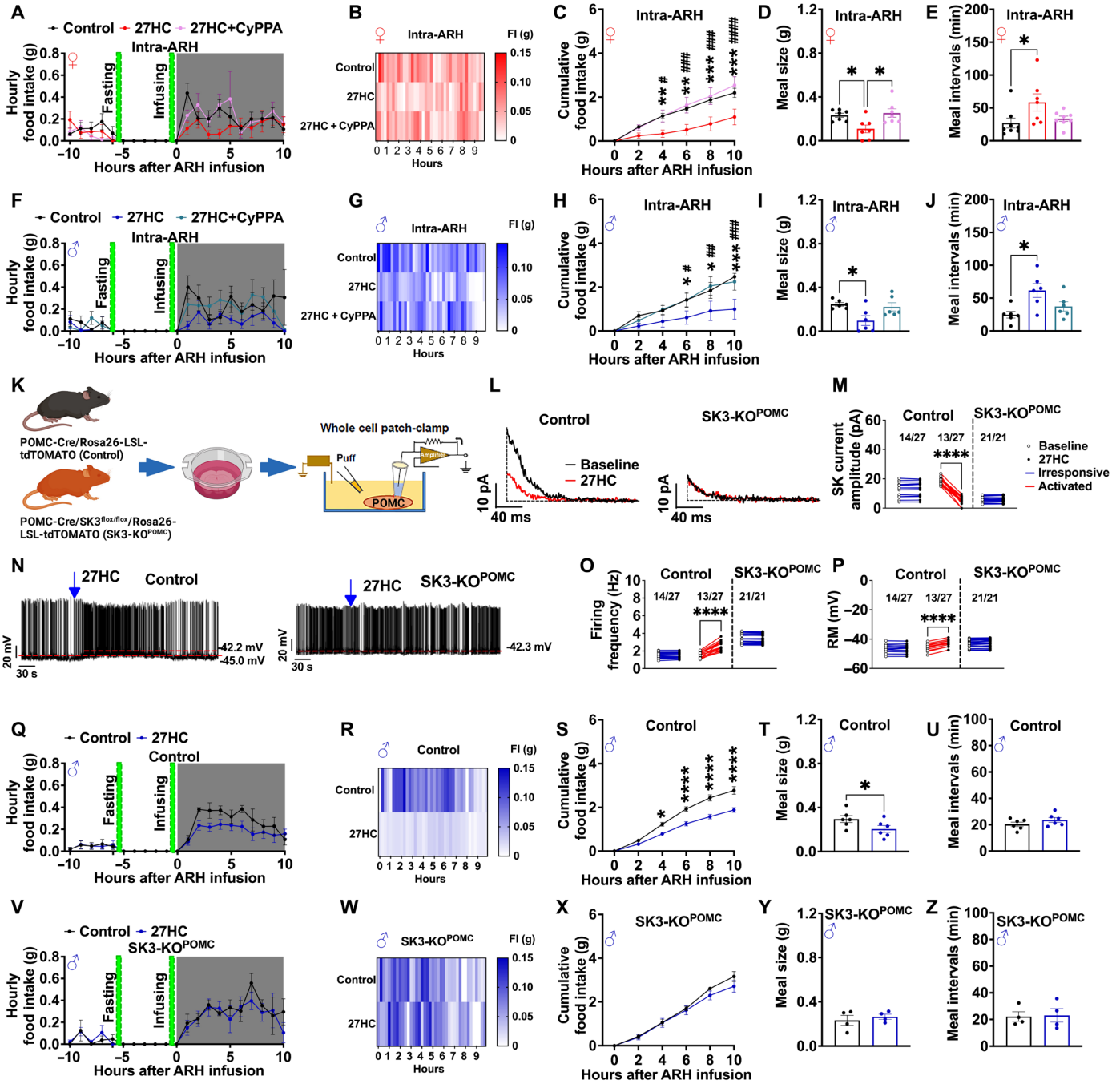

Fig. 8. SK3 mediates 27HC's actions to stimulate POMC^{ARH} neurons and inhibit food intake. (**A** to **J**) Dark-induced food intake of 12-week C57BL/6J female mice [(A) to (E), $n = 6$] and male mice [(F) to (J), $n = 6$] after intra-ARH infusion of vehicle, 0.1 nmol 27HC, or 0.1 nmol 27HC + 0.025 pmol CyPPA. Hourly food intake [(A) and (F)], a heatmap of food consumption [(B) and (G)], cumulative food intake [(C) and (H)], mean meal size [(D) and (I)], and mean intermeal intervals [(E) and (J)] 10 hours after infusion. (**K**) Schematic of electrophysiology recordings of POMC-Cre/Rosa26-LSL-tdTOMATO (Control) or POMC-Cre/*Kcnn3*$^{flox/flox}$/Rosa26-LSL-tdTOMATO mice (SK3-KO^{POMC}). (**L** and **M**) Representative traces (L) and data analysis (M) of SK current in POMC^{ARH} neurons from control or SK3-KO^{POMC} mice after 27HC puff treatment (1 s, 100 nM; $n = 27$ or 21 from three different animals in each group). (**N** to **P**) Representative traces (N) and data analysis of resting membrane potential (O) and firing frequency (P). (**Q** to **Z**) Dark-induced food intake of 12-week male *Kcnn3*$^{flox/flox}$ Control, (Q) to (U), $n = 6$] and male POMC-Cre/*Kcnn3*$^{flox/flox}$ mice [SK3-KO^{POMC}, (V) to (Z), $n = 6$] after intra-ARH infusion of vehicle or 0.1 nmol 27HC. Results are shown as means ± SEM. [(C), (H), and (S)] $^{*}P < 0.05$, $^{**}P < 0.01$, $^{***}P < 0.001$, and $^{****}P < 0.0001$ (27HC versus Control) or $^{\#}P < 0.05$, $^{\#\#}P < 0.01$, $^{\#\#\#}P < 0.001$, and $^{\#\#\#\#}P < 0.0001$ (27HC + CyPPA versus 27HC) indicate statistical significance in two-way ANOVA followed by post hoc Sidak tests. [(D), (E), (I), and (J)] $^{*}P < 0.05$ indicates statistical significance in one-way ANOVA followed by post hoc Tukey tests. [(M), (O), and (P)] $^{****}P < 0.0001$ indicates statistical significance in paired *t* tests. (T) $^{*}P < 0.05$ indicates statistical significance in unpaired *t* tests.

modeling (*82*, *83*) are necessary to quantitatively assess the specific response of dynamic substrate utilization to 27HC treatment under various conditions.

Notably, the intraperitoneal injection dose of 27HC (20 mg/kg) has been previously shown to increase circulating 27HC within the physiological range, but it did not affect circulating cholesterol levels (*21*, *22*, *46*). Consistently, the central delivery of 0.1 nmol of 27HC is well within the daily flux of 12 μmol (5 mg) of 27HC from the circulation into the brain in humans (*24*), and the estimated daily flux of 4 μmol of 27HC in mice (*24*, *46*, *78*). Considering the strong correlation between circulating cholesterol and 27HC levels, the results also suggest that, physiologically, 27HC may function as a negative feedback signal induced by postprandial cholesterol surge to inhibit food intake and prevent further increases in blood cholesterol levels. A similar negative feedback theory has been proposed for 27HC, which acts on LXRs to stimulate cholesterol elimination and RCT in peripheral tissues in response to cholesterol overload (*18*, *84*).

Furthermore, it is essential to note that intraperitoneal and intracerebroventricular injections of 27HC rapidly decreased food intake within the first few hours. Despite its high lipophilicity, which allows it to cross cell membranes and the BBB passively, 27HC may still require time to penetrate brain tissue. The intriguing observation is that intraperitoneal and intracerebroventricular injections exhibit similar timelines in suppressing food intake despite using different routes to reach the brain tissue. One possible explanation is that 27HC bypasses the BBB and directly affects the ARH near the median eminence. The median eminence lacks the typical BBB and acts as a pathway for the ARH to receive metabolic signals, such as leptin and ghrelin, reflecting the body's nutritional status (*85*–*88*). Therefore, it is possible that some circulating 27HC can quickly reach the ARH through the permeable median eminence, bypassing the BBB. However, additional research is required to confirm this hypothesis.

The intracerebroventricular doses of 27HC (0.01 or 0.1 nmol) that elicited significant anorexigenic responses in both males and females are considerably lower than the estimated daily flux of 27HC from the bloodstream into the brain in mice, which is 4 μmol (*24*, *75*). This raises questions about how these low doses of 27HC can have any anorexigenic effects when they are much lower than the normal physiological levels. Notably, the daily flux does not reflect the actual 27HC dose in the brain. Previous studies have shown that the brain can convert 27HC into more polar products, effectively acting as a metabolic "sink" (*24*). The essential process in the metabolism of 27HC in the brain is catalyzed by CYP7B1, which is present at an exceptionally high level in the brain (*89*). These findings suggest that the effective daily flux of 27HC in mice is likely much lower than 4 μmol, which helps explain why low doses of 27HC (0.001 to 0.1 nmol) given through intracerebroventricular administration have a significant effect.

In addition, in our study, we administered 27HC through intracerebroventricular or intra-ARH injection, allowing 27HC to diffuse directly within the cerebrospinal fluid (CSF) or ARH. With intracerebroventricular administration, doses of 0.001 to 0.1 nmol of 27HC would theoretically result in a final concentration of 25 nM to 2.5 μM 27HC in the CSF, based on the total volume of 40 μl of CSF in mice (*90*). The final concentration may be even higher with intra-ARH injection. These concentrations fall within the effective range (100 nM or higher) needed to activate POMC neurons, as shown by electrophysiological recording.

The data from our pharmacological blockade experiments and ERα-KO^{POMC} model further demonstrate the necessity of ERα expressed by POMC neurons in the regulatory effects of 27HC on feeding behavior. Notably, the following chemogenetic activation of POMC^{ARH} blocked the effects of 27HC on feeding behavior, suggesting POMC^{ARH}-induced hypophagia. These results indicate that the anorexigenic effects of 27HC are at least partially mediated through ERα-dependent activation of POMC^{ARH} neurons. Notably, besides ARH, the POMC-Cre mouse line has been shown to direct recombination in other brain regions that are implicated in energy homeostasis, including NTS, the paraventricular nucleus of the hypothalamus (PVN), the ventromedial nucleus of the hypothalamus (VMH), subiculum, medial amygdala (MeA), the lateral parabrachial nucleus (LPB), and area postrema (AP) (*91*). The attenuation of 27HC's anorexigenic effects in the ERα-KO^{POMC} model could be partially attributed to ARH-independent ERα deletion. Similarly, the inhibitory effect of intracerebroventricularly infused E2 on food intake was abolished in the ERα-KO^{POMC} model, this confirm the regulatory role of ERα in ARH in feeding behavior. Among these brain regions, ERα is absent or barely expressed in the PVN (*92*–*94*). Genetic deletion of ERα in the MeA or VMH does not modulate feeding behavior (*52*, *92*, *95*). However, NTS, LPB, and AP are critical nuclei for the regulation of feeding behavior, and NTS, subiculum, LPB, and AP do express high levels of ERα (*96*–*100*). In addition, recent studies also demonstrated that subiculum circuits integrate hunger state signals to regulate the decision to eat (*101*, *102*). Thus, it will be interesting to validate whether 27HC could act on ERα neurons in NTS, subiculum, LPB, or AP to modulate feeding behavior.

Consistent with previous findings (*60*, *103*, *104*), a single bolus intracerebroventricular injection of E2 acutely reduced food intake in both male and female control mice. However, similar to 27HC, the appetite-suppressing effects of centrally delivered E2 were blocked in male and female ERα-KO^{POMC} mice. This suggests that the acute anorexigenic effects of E2 primarily occur through ERα expressed by POMC neurons. However, this does not rule out the potential role of other brain ERα in different forms of estrogenic regulation of food intake, such as chronic appetite-suppressing effects or appetite regulatory response during metabolic adaptations to temperature (*105*) or nutritional challenges (*106*). Further clarification is needed to determine the specific physiological role of other brain ERα in the regulation of food intake.

Another intriguing finding is that although our evidence supports a mediating role of POMC^{ARH} in acute anorexigenic effects of 27HC, chemogenetic activation of POMC^{ARH} neurons does not rapidly decrease food intake but instead leads to a reduction of daily food intake after the second dose of 27HC central delivery. This is consistent with previous observations that acute stimulation of the POMC^{ARH} population does not produce the canonical reduction in food intake (*63*, *107*–*109*), despite the well-known anorexigenic effects of α-MSH. Optogenetic and chemogenetic activation of POMC^{ARH} appears to suppress chronic daily feeding instead (*63*, *108*). This discrepancy could be explained by the heterogeneity of the POMC^{ARH} neural population. Although POMC^{ARH} neurons have been considered a homogeneous population, previous studies have highlighted the functional diversity attributed to distinct downstream circuits, translational signatures, electrophysiological properties, neurotransmitters, and energy state–sensing signals (*110*). Using intersectional chemogenetic targeting technology, it was recently shown that activation of POMC^{ARH} neurons coexpressing glucagon-like peptide 1 receptor resulted in early onsite (2.5 hours after CNO injection) and potent feeding suppression (*110*). Conversely, activation of POMC^{ARH} neurons has also been shown to promote food intake by releasing the opioid peptide β-endorphin as a neurotransmitter (*111*, *112*). The acute anorexigenic effect of 27HC

could be mediated by a subpopulation of POMC^{ARH} neurons that express ERα and exert a rapid hypophagic response.

The hypophagia induced by central 27HC delivery seems contradictory to a previous finding that chronic systemic administration of 27HC (for 8 weeks) promotes adiposity by increasing white adipose tissue inflammatory responses in an ERα-dependent mechanism (*46*). However, the previous results do not rule out the possibility of acute central anorexigenic effects of 27HC. Notably, 27HC has been shown to act as a SERM with mixed estrogenic bioactivities (i.e., agonist or antagonist) in different tissues (*17*, *20*, *21*). Cumulative evidence has demonstrated that 27HC acts as an agonist of ERα, facilitating metastasis and promoting tumor growth in breast cancer (*113*, *114*). Meanwhile, 27HC functions as an antagonist of ERs, preventing the estrogenic cardioprotective effects in vivo (*21*, *22*). These mixed ER responses suggest that the complex of 27HC and ERα expressed by POMC^{ARH} would have a distinct role in energy homeostasis compared with 27HC and ERα in white adipose tissue. Similarly, tamoxifen is widely used to treat all stages of ERα-positive breast cancer, presenting its antagonist role with ER (*115*). Tamoxifen mimics E2's effect of reducing food intake and body weight gain in ovariectomized rats (*116*). Therefore, additional studies are needed to investigate further the mechanisms of the potential "conflicted" roles of 27HC in different tissues in the regulation of energy homeostasis.

We further investigated the intracellular mechanism of 27HC-induced stimulation on POMC^{ARH} neurons and its effects on feeding behavior. Our findings show that 27HC activates POMC^{ARH} neurons in an SK3-dependent manner. The 27HC-induced hypophagia is blocked by pharmacological activation of SK current or genetic deletion of SK3 in the POMC neurons, suggesting that SK3 mediates POMC^{ARH} activation, and following the anorexigenic effects of 27HC. Previously, we reported that SK3 is the most abundant isoform of SK channels in POMC^{ARH} and regulates energy and glucose homeostasis in a sexually dimorphic manner (*64*). SK3 in POMC^{ARH} neurons regulates food intake and physical activity in male mice and glucose balance in female mice, respectively (*64*). However, this is inconsistent with our observations that 27HC shows similar anorexigenic effects in both male and female mice. If SK3 is the downstream mediator for 27HC's effects on POMC^{ARH} neurons, we would expect the same sex-dimorphic metabolic responses. This discrepancy could be due to the functionally heterogeneous effects of POMC^{ARH} neurons on feeding. Our data support the mediating roles of both ERα and SK3 in the regulatory effects of 27HC on POMC^{ARH} neurons. Therefore, 27HC's metabolic responses require SK3 + ERα + POMC^{ARH} neurons instead of SK3 + POMC^{ARH} neurons. It is worth pursuing whether a subpopulation of POMC neurons, such as SK3 + ERα + POMC^{ARH} neurons, represents a functionally segregated POMC population that rapidly modulates food intake and mediates a negative feedback function of 27HC to reduce prandial cholesterol surging.

A clear sex dimorphic response has been observed in mice treated with a low dose of 27HC (0.001 nmol). This response may be attributed to the higher expression of ERα in the POMC^{ARH} neurons in females, as demonstrated by colocalization analysis of POMC-tdTOMATO and ERα-ZsGreen. These findings are consistent with previous reports that females have more POMC^{ARH} neurons than males (*117*) and that ERα mRNA expression in ARH is greater in females than in males (*118*). Our recent data showed that male ERα + POMC^{ARH} neurons have a significantly higher SK current than female ERα + POMC^{ARH} neurons (*64*). This suggests a relatively higher ceiling effect for the 27HC-induced stimulation on POMC^{ARH} neurons in males. It may compensate for the higher expression of ERα and greater POMC neurons in females and explain why we did not observe a remarkable sexual difference in the anorexigenic response to the acute 27HC treatment. Further complicating matters is that CYP7B1, the enzyme responsible for catalyzing 27HC and primarily expressed in the brain (*89*, *119*, *120*), is negatively regulated by androgens and positively up-regulated by estrogens (*121*, *122*). This suggests that the cumulative level or half-life of 27HC in the brain may differ between males and females, potentially affecting the duration of the feeding response induced by 27HC treatment.

In summary, our results support a model in which 27HC, the most abundant metabolite of cholesterol, produces acute anorexigenic effects by activating POMC^{ARH} neurons via ERα/SK3 signaling. Because circulating levels of 27HC and cholesterol are tightly correlated, 27HC may act as a peripheral cholesterol indicator and transmit nutritional signals to the brain to inhibit feeding and prevent further increases in circulating cholesterol. Identifying this previously unknown negative feedback mechanism is a significant step forward in our understanding of mammalian energy and cholesterol homeostasis. It also provides an additional target for pharmacological manipulation to treat obesity and metabolic syndrome.

MATERIALS AND METHODS

Mice

Several transgenic mouse lines were maintained on a C57BL/6J background. These lines include *Esr1*$^{flox/flox}$ (*123*), POMC-Cre (catalog no. 005965, The Jackson Laboratory, Bar Harbor, ME, USA), Rosa26-LSL-tdTOMATO (catalog no. 007914, The Jackson Laboratory), *Kcnn3*$^{flox/flox}$ (catalog no. 019083, Jackson Laboratory), and ERα-ZsGreen (*50*). C57BL/6J male and female mice were purchased from The Jackson Laboratory (catalog no. 000664). ERα-ZsGreen, POMC-Cre, and Rosa26-LSL-tdTOMATO were crossed to generate ERα-ZsGreen/POMC-Cre/Rosa26-LSL-tdTOMATO for ERα and POMC colocalization analysis. POMC-Cre, Rosa26-LSL-tdTOMATO, and *Kcnn3*$^{flox/flox}$ were crossed to generate POMC-Cre/tdTOMATO or *Kcnn3*$^{flox/flox}$/POMC-Cre/Rosa26-LSL-tdTOMATO (SK3-KO^{POMC}) for electrophysiological recording and immunohistochemistry staining. *Esr1*$^{flox/flox}$ mice were crossed with POMC-Cre to generate *Esr1*$^{flox/flox}$/POMC-Cre (ERα-KO^{POMC}) to specifically knock out *Esr1* in the POMC neurons. *Kcnn3*$^{flox/flox}$ mice were crossed with POMC-Cre to generate *Kcnn3*$^{flox/flox}$/POMC-Cre (SK3-KO^{POMC}) to specifically knock out *Kcnn3* in the POMC neurons. Mice were housed in a temperature-controlled environment at 22° to 24°C on a 12-hour light/12-hour dark cycle (6 a.m. and 6 p.m.) or 14-hour light/10-hour dark cycle (5 a.m. and 7 p.m.). Unless otherwise stated, the mice were fed ad libitum with standard mouse chow (6.5% fat: catalog no. 2920, Harlan-Teklad, Madison, WI, USA) and water. Care of all animals and procedures were approved by Pennington Biomedical Research Center (PBRC), Baylor College of Medicine, and The University of Illinois at Chicago Institutional Animal Care and Use Committees.

Feeding behavior test

Feeding behavior was studied using the BioDAQ Food Intake Monitor for mice (BioDAQ, Research Diets Inc., New Brunswick, NJ, USA), which allows continuous monitoring of meal patterns in undisturbed mice with minimal human interference. All the mice were habituated for 1 week to single housing and fed with standard chow through a BioDAQ food hopper in regular housing cages with environmental

enrichment and bedding material. Water was provided ad libitum from a BioDAQ Stainless Steel LIQUID Hopper. Mice were fasted for 6 hours before the initiation of the dark cycle (7 p.m.). At the beginning of the dark cycle, mice received an intraperitoneal injection of vehicle (9% 2-hydroxypropyl-β-cyclodextrin in saline) or 27HC (20 mg/kg; 1 mg/ml in vehicle with a dose of 10 μl/g body weight, catalog no. SML2042, MilliporeSigma, Burlington, MA, USA). Food intake was continuously measured for 10 hours after injections.

In separate cohorts of male and female C57BL/6J mice, an indwelling intracerebroventricular guide cannula with 2.3-mm projection (catalog no. 62003, P1 Technologies, Roanoke, VA, USA) was stereotaxically inserted to target the lateral ventricle (bregma, anterior-posterior: −0.4 mm; lateral: +1.3 mm; dorsalventral: −2.3 mm) (*124*). One week after surgery, the cannulation accuracy was validated by the increase of drinking and grooming behavior after intracerebroventricular administration of 10 ng of angiotensin II (10 μg/ml in saline, RP11257, GenScript Biotech, Piscataway, NJ, USA), as we did before (*125*, *126*). After validation, the mice went through a 6-hour fasting before the dark cycle. The dark-induced food intake was measured after intracerebroventricular injection of vehicle or 0.1 nmol 27HC (100 μM in 1 μl of vehicle) at the beginning of the dark cycle.

To determine whether ERα or MC3/4R in the brain is required for the orexigenic effects of 27HC, male and female C57BL/6J mice were subjected to the same procedure but received intracerebroventricular injections of vehicle, 0.1 nmol 27HC, 250 nmol BHPI (250 mM in 1 μl of vehicle, catalog no. 5380050001, MilliporeSigma), 6 nmol SHU 9119 (6 mM in 1 μl of vehicle, HY-P0227, MedChemExpress, Monmouth Junction, NJ, USA), 0.1 nmol 27HC + 250 nmol BHPI, or 0.1 nmol 27HC + 6 nmol SHU 9119, which were tested in another cohort of male and female C57BL/6J mice.

To determine whether ERα expressed by POMC neurons mediates orexigenic effects of 27HC, male and female control (*Esr1*$^{flox/flox}$) or ERα-KO^{POMC} (*Esr1*$^{flox/flox}$/POMC-Cre) mice were implanted with a guide cannula targeting later ventricular and received intracerebroventricular injections of vehicle, 0.1 nmol 27HC, or 5 μg cyclodextrin-encapsulated 17β-estradiol (5 mg/ml E2 in 1 μl of vehicle, E4389, MilliporeSigma).

To test the requirement of ERα in the ARH, female *Esr1*$^{flox/flox}$ mice at 8 weeks of age were bilaterally injected with 100 nl of AAV-CMV-EGFP (UNC Vector Core, control) or AAV-CMV-Cre-GFP (UNC Vector Core, ERα-KO^{ARH}) into the ARH (bregma, anterior-posterior: −1.6 mm; lateral: +0.30 mm; dorsal-ventral: −5.9 mm). Under the same anesthesia, all mice were implanted with an intracerebroventricular cannula that targeted the lateral ventricle. Four weeks after the surgery, the mice were then intracerebroventricularly infused with either vehicle or 0.1 nmol 27HC (100 μM in 1 μl of vehicle), and their feeding behavior was investigated as described above. After the injections, all mice were perfused, and their brains were collected. The brains were sectioned and mounted, and the Cre-GFP signals were monitored under a fluorescent microscope to validate the virus injection accuracy. Another aliquot of brain sections was used for immunohistochemistry of ERα. Briefly, brain sections were incubated with rabbit anti-ERα antibody (1:10,000; catalog C1355, MilliporeSigma) at room temperature overnight, followed by the biotinylated donkey anti-rabbit secondary antibody (1:1000, catalog no. 711-067-003, Jackson ImmunoResearch) for 2 hours. Sections were then incubated in the avidin-biotin complex (1:1000, PK-6100, Vector Laboratories) and incubated in 0.04% 3,3′-diaminobenzidine and 0.01% hydrogen peroxide. After dehydration through graded ethanol, the slides were then immersed in xylene and coverslipped. Bright-field images were obtained using a Leica DM5500 microscope.

To investigate whether 27HC promotes feeding by inhibiting SK current in the ARH, male and female C57BL/6J mice were implanted with a guide cannula with a 5.9-mm projection to target the ARH (bregma, anterior-posterior: −1.7 mm; lateral: +0.25 mm; dorsal-ventral: −5.9 mm). Specifically, the mice were infused with vehicle, 0.1 nmol 27HC (200 μM in 0.5 μl of vehicle), 0.025 pmol CYPPA (50 nM in 0.5 μl of vehicle, C5493, MilliporeSigma), or 0.1 nmol 27HC + 0.025 pmol CYPPA in the ARH.

To investigate whether SK3 expressed by POMC neurons mediates the orexigenic effects of 27HC, male control (*Kcnn3*$^{flox/flox}$) or SK3-KO^{POMC} (*Kcnn3*$^{flox/flox}$/POMC-Cre) mice were implanted with a guide cannula targeting the ARH. The mice were then infused with vehicle or 0.1 nmol 27HC (200 μM in 0.5 μl of vehicle) in the ARH.

c-Fos mapping after 27HC treatment

Male and female ERα-ZsGreen mice were implanted with an intracerebroventricular cannula targeting the lateral ventricle, as previously described. After fasting for 6 hours, the mice received an intracerebroventricular infusion of either vehicle (1 μl, 9% 2-hydroxypropyl-β-cyclodextrin in saline) or 27HC (1 μl, 100 μM in vehicle) at 7 p.m., the start of the dark cycle. All mice were perfused 1.5 hours after infusion. The brains were collected and sectioned into 30-μm slices. The sections were blocked with 3% normal goat serum for 1 hour, then incubated overnight on a shaker at room temperature with c-Fos (9F6) Rabbit mAb (1:1000, 2250S, Cell Signaling Technology), followed by incubation with Goat Anti-Rabbit Alexa Fluor 594 IgG (H + L) (1:500, 1110585-003, Jackson ImmunoResearch) for 2 hours. Slides were coverslipped using an anti-fade mounting medium (H-1500, Vector Laboratories, Newark, CA, USA), and fluorescence images were captured using a Leica DM5500 fluorescence microscope. ERα-ZsGreen neurons coexpressing c-Fos were counted and averaged in at least five consecutive coronal brain slices containing the arcuate nucleus from each mouse, and these data were treated as one biological sample. Statistical analyses were performed using data from three different mice.

The same procedure was also performed on the overnight-fasted control and ERα-KO^{POMC} mice to examine c-Fos expression in the ARH after intracerebroventricular injection of 27HC.

Metabolic phenotyping of mice

Indirect calorimetry measurements were performed using the Promethion metabolic cage system (Sable Systems International, Las Vegas, NV, USA) located at the Biologic Resources Laboratory at the University of Illinois at Chicago. Before data acquisition, the mice were acclimatized for 72 hours in the Promethion system and fed ad libitum with standard mouse chow and water. Instrument control and data acquisition followed the manufacturer's instructions. Like the feeding behavioral tests, male and female C57BL/6J mice were implanted with a guide cannula targeting the lateral ventricle and underwent a 6-hour fast before the dark cycle. Food intake, energy expenditure, and substrate utilization were measured after intracerebroventricular injection of either vehicle or 0.1 nmol 27HC at the beginning of the dark cycle. Raw data were processed using ExpeData software (Sable Systems), and calorimetric analysis was

performed using a free online tool called CalR (https://calrapp.org) (*127*).

To determine whether the changes induced by 27HC in the whole-body substrate utilization are independent of its inhibitory effects on food intake, we implanted an intracerebroventricular guide cannula in another cohort of male and female C57BL/6J mice, as previously described. After a 2-week postsurgical observation period, the mice underwent 4 days of intermittent fasting training before metabolic chamber recording. During the training period, the mice were only allowed access to the chow diet between noon and 6:00 p.m., and body weight and food intake were measured before starting the fasting cycle. This feeding schedule was maintained during the subsequent indirect calorimetry test, and intracerebroventricular infusions were performed immediately after the 6-hour re-feed period.

To investigate the regulatory effects of 27HC on whole-body substrate utilization in the fasting condition, a separate cohort of female C57BL/6J mice was implanted with an intracerebroventricular cannula and acclimated to the Promethion metabolic cage system. intracerebroventricular infusions were administered immediately following an 18-hour overnight fast.

ERα colocalization with POMC neurons

To map the collocation of ERα and POMC neurons, we generated ERα-ZsGreen/POMC-Cre/Rosa26-LSL-tdTOMATO mice by crossing ERα-ZsGreen, POMC-Cre, and Rosa26-LSL-tdTOMATO mice. In these mice, POMC-positive cells were labeled by tdTOMATO fluorescence, and ERα-positive cells were labeled by ZsGreen fluorescence. Male and female ERα-ZsGreen/POMC-Cre/Rosa26-LSL-tdTOMATO mice were perfused at 8 weeks of age, and brain sections were cut at 30 μm after perfusion. The sections were then mounted and coverslipped with an anti-fade mounting medium, and fluorescence images were captured using a Leica DM5500 fluorescence microscope.

Secondary analysis of scRNA-seq results

Counts and metadata were downloaded from GSE93374. The count data were normalized to counts per million (CPM) and filtered for cells in the ARH (*109*). Next, the count data were joined to the metadata by cell ID. Genes such as LXRα-β and POMC were selected and exported to an Excel file. Further filtering was applied in Excel using metadata or expression data. We extracted the expression profiles of LXRα-β and POMC in neurons only and compared the expression of LXRα and LXRβ in POMC neurons.

Knockdown of LXRβ in POMC^{ARH} neurons during adulthood

The CRISPR-Cas9 approach was used to selectively disrupt LXRβ in POMC^{ARH} neurons bilaterally, as previously reported (*128*). At 8 weeks of age, both male and female POMC-Cre mice and their WT littermates received bilateral stereotaxic injections of 200 nl of AAV/DJ-CMV7-DIO-saCas9 (7122, Vector Biolabs, Malvern, PA, USA) mixed with AAV-LXRβsgRNA-DIO-mCherry (1:5 volume ratio) into the ARH region (bregma, anterior-posterior: −1.6 mm; lateral: +0.30 mm; dorsal-ventral: −5.9 mm). LXRβsgRNA (GGCAGCGGAACCTGCCAG) against LXRβ was designed and validated using the UCA method based on the single-strand annealing mechanism (*129*) by Biocytogen (Wakefield, MA, USA) before being cloned and packaged into AAV-LXRβsgRNA-DIO-mCherry vector (Baylor College of Medicine Viral Vector Production Core, Houston, TX, USA). LXRβsgRNA was expressed in all infected cells, and Cas9 protein was expressed in Cre-positive cells in the POMC-Cre mice. A portion of POMC^{ARH} neurons that coexpressed both LXRβsgRNA and Cas9 protein had LXRβ mutated. Not all POMC^{ARH} neurons were infected with both viruses; thus, LXRβ was not completely mutated in all POMC^{ARH} neurons. As a result, these mice were referred to as POMC-LXRβ knockdown (LXRβ-KD^{POMC}) mice instead of knockout mice. LXRβ was not mutated in POMC neurons of the WT mice that only expressed LXRβsgRNA, referred to as controls. After the surgery, all mice were fed a chow diet for 9 weeks before being switched to a high-fat diet (60% fat diet, catalog no. D12492, Research Diets). Body weight and food intake were measured every 4 days. Glucose tolerance tests (GTTs) were performed at weeks 8 and 18 after the virus injection, and insulin tolerance tests (ITTs) were performed at weeks 9 and 19 after the virus injection. In GTT, overnight-fasted mice were intraperitoneally injected with D-glucose (1 g/kg, catalog no. D9434, US Pharmacopeia pharmaceutical grade, MilliporeSigma), and tail blood glucose was measured using a true-test glucometer immediately before and 15, 30, 60, and 120 min after injection. In ITT, fed mice were intraperitoneally injected with insulin (1 U/kg, Humulin R; Eli Lilly Corp., Indianapolis, IN), and tail blood glucose was measured using a true-test glucometer immediately before and 15, 30, 60, and 120 min after injection.

To further investigate the role of LXRβ expressed by POMC^{ARH} neurons in the hypophagic effects of 27HC, another cohort of male control and LXRβ-KD^{POMC} mice was generated, as explained earlier. These mice were implanted with a guide cannula targeting the lateral ventricle. Afterward, the mice were intracerebroventricularly infused with either vehicle or 0.1 nmol 27HC (100 μM in 1 μl of vehicle) in the ARH. Eating behaviors were investigated using the methods described previously.

Validation of LXRβ recombination in POMC^{ARH} neurons

To determine if the CRISPR-Cas9 system had successfully induced the mutation of LXRβ, a two-step PCR was conducted. Each reaction contained a single POMC neuron that was handpicked under the microscope (*35*, *105*). The sgRNA target region of LXRβ and a nonrelevant region of the genome were amplified in a two-step nested PCR. For the first step of PCR, the primer pair across the sgRNA target region of LXRβ: 5′-GGCTTTTGATTCTTGGGGCG-3′ and 5′-GTTCAGCTCTGGTCTCGTCC-3′ (2.2 kb) was used. To ensure that the neuron picking was successful, a control primer pair (sense: 5′-GGTCAGCCTAATTAGCTCTGTCAT-3′ and 5′-GATCTCCAGCTCCTCCTCTGTCT-3′) was also included to amplify the nonrelevant region of the genome (600 bp). The PCR products were then used for the second step of PCR with another LXRβ primer pair: 5′-CGGGTAGCCTGAGCTGTATG-3′ and 5′-TAGGAAACCCCTCCCTAGCC-3′ (1.3 kb) and control primers (600 bp).

DREADD manipulation of POMC^{ARH} neuron

To determine whether POMC^{ARH} neuron activation is necessary for the anorexigenic effect induced by 27HC, female and male POMC-Cre mice were bilaterally injected with 200 nl of AAV-EF1a-DIO-mCherry (UNC Vector Core) or AAV-EF1a-DIO-hM4D(Gi)-mCherry (Stanford Gene Vector and Virus Core) into the ARH at 8 weeks of age. At the same time, a guide cannula (62003 with a terminal length of 3.5 mm; RWD Life Science, Guangdong, China) was implanted to target the lateral ventricle. An internal cannula (62203, customized to fit 3.5-mm 62003 with 0.5-mm projection, RWD Life Science) was used

for drug infusion. Two weeks after surgery, following a brief 6-hour fast, the mice received one of four treatments before the dark cycle: vehicle (9% 2-hydroxypropyl-β-cyclodextrin in saline), 1 μg of CNO (1 μg/μl in 1 μl of vehicle), 0.1 nmol 27HC (100 mM in 1 μl of vehicle), or 1 μg of CNO + 0.1 nmol 27HC. Feeding behavior was continuously monitored by the BioDAQ system during the experimental phase. The order of infusion was randomized to avoid "sequence effects," and each trial was separated by 72 hours to ensure the "wash out" of the previous infusion. After the injections, all mice were perfused, and their brains were collected. The brains were sectioned and mounted, and the mCherry signals were monitored under a fluorescent microscope to validate the virus injection accuracy. Only mice with mCherry signals exclusively in the ARH were included in the analyses for feeding behavior.

Electrophysiology

We investigated the electrophysiological responses of identified POMC neurons in the ARH to 27HC treatment in POMC-Cre/tdTOMATO mice, as previously described (*64*, *65*). To do so, we performed whole-cell patch-clamp recordings on identified red fluorescent neurons in brain slices containing ARH from POMC-Cre/tdTOMATO mice. We used mice that were 6 to 12 weeks old, and they were deeply anesthetized with isoflurane and transcardially perfused with a sucrose-based cutting solution (pH 7.3) that was ice-cold and carbogen-saturated (95% O_2, 5% CO_2). The solution contained 10 mM NaCl, 25 mM $NaHCO_3$, 195 mM sucrose, 5 mM glucose, 2.5 mM KCl, 1.25 mM NaH_2PO_4, 2 mM Na pyruvate, 0.5 mM $CaCl_2$, and 7 mM $MgCl_2$. We removed the entire brain and coronally cut it into slices (250 μm) using a Leica vibratome (1200s, Leica Biosystems). Then, we incubated the ARH-containing slices in oxygenated artificial CSF (aCSF; adjusted to pH 7.3) containing 126 mM NaCl, 2.5 mM KCl, 2.4 mM $CaCl_2$, 1.2 mM NaH_2PO_4, 1.2 mM $MgCl_2$, 11.1 mM glucose, and 21.4 mM $NaHCO_3$ for 1 hour at 34°C.

Slices were transferred to a recording chamber and perfused with oxygenated aCSF at a flow rate of 1.8 to 2 ml/min at 34°C. tdTOMATO-labeled $POMC^{ARH}$ neurons were visualized using epifluorescence and IR-DIC imaging. The intracellular solution (adjusted to pH 7.3) contained the following: 128 mM K gluconate, 10 mM KCl, 10 mM Hepes, 0.1 mM EGTA, 2 mM $MgCl_2$, 0.05 mM Na-GTP, and 0.05 mM Mg-ATP. Recordings were made using a MultiClamp 700B amplifier (Molecular Devices, Sunnyvale, CA, USA), sampled using Digidata 1440A, and analyzed offline with pClamp 10.3 software (Molecular Devices). Series resistance was monitored throughout the recording and was generally less than 10 megohms, without compensation. The liquid junction potential (LJP) was +12.5 mV and was corrected after the experiment. Data were excluded if the series resistance increased dramatically during the experiment or if there was no overshoot for the action potential. Currents were amplified, filtered at 1 kHz, and digitized at 20 kHz. The current clamp was used to test neuronal firing and resting membrane potential before and after a 1-s puff of aCSF containing 0, 1 nM, 10 nM, 100 nM, 1 μM, or 10 μM 27HC.

To test whether 27HC directly stimulates $POMC^{ARH}$ neurons, brain slices were treated with 100 nM 27HC after preincubation with an aCSF solution containing 1 μM TTX, a sodium channel blocker (catalog no. 1078, R&D Systems, Minneapolis, MN, USA), and a cocktail of fast synaptic inhibitors. The cocktail included bicuculline (50 μM), a GABA receptor antagonist (catalog no. 0130, Tocris, Minneapolis, MN, USA), AP-5 (30 μM), an NMDA receptor antagonist (catalog no. 0106, Tocris), and CNQX (30 μM), an AMPA receptor antagonist (catalog no. 0190, Tocris) to block most presynaptic inputs. AP-5 (30 μM) and CNQX (30 μM) were used to block glutamatergic inputs, while bicuculline (50 μM) was included to block GABAergic inputs. To test whether ERα or ERβ is necessary for the stimulatory effects of 27HC on $POMC^{ARH}$ neurons, brain slices were treated with 100 nM 27HC in the presence of TTX, a cocktail of synaptic inhibitors, and either BHPI (50 μM), an ERα antagonist (catalog no. 5.38005, MilliporeSigma), or PHTPP (10 μM), an ERβ antagonist (catalog no. 2662, Tocris).

In some experiments, apamin-sensitive outward tail currents (SK currents) were recorded following previously described methods with some modifications (*130*, *131*). SK currents in $POMC^{ARH}$ neurons were recorded under a voltage clamp in the presence of TTX. A 400-ms depolarizing pulse was applied (from −60 to 0 mV and back to −60 mV, holding at −60 mV) (*130*–*132*).

To determine the role of SK3 expressed by $POMC^{ARH}$ neurons, we crossed POMC-Cre, Rosa26-LSL-tdTOMATO, and $Kcnn3^{flox/flox}$ to generate POMC-Cre/tdTOMATO or $Kcnn3^{flox/flox}$/POMC-Cre/Rosa26-LSL-tdTOMATO ($SK3\text{-}KO^{POMC}$) mice for electrophysiological recording. The electrophysiology recordings of tdTOMATO-labeled $POMC^{ARH}$ neurons were performed when the mice were 6 to 8 weeks old. Mice were allowed to eat ad libitum. On the day of recording, the fed mice were deeply anesthetized with isoflurane and transcardially perfused. Brain slices containing the ARH were prepared and maintained in aCSF, as described above.

Validation of *Kcnn3* deletion in $POMC^{ARH}$ neurons

At 9 a.m., male $Kcnn3^{flox/flox}$/POMC-Cre/Rosa26-LSL-tdTOMATO and POMC-Cre/tdTOMATO mice were anesthetized with inhaled isoflurane and perfused with saline, followed by 10% formalin. Brain sections (30 μm thick) were collected and subjected to immunofluorescent staining for SK3.

Briefly, the sections were blocked with 5% normal donkey serum for 1 hour, then incubated overnight with rabbit anti-SK3 antibody (1:500 dilution; catalog no. APC-025, Alomone Labs) on a shaker at room temperature. The next day, the brain sections were incubated with donkey anti-rabbit Alexa Fluor 488 (1:500; catalog no. A21206, Invitrogen) for 2 hours. Slides were coverslipped using an anti-fade mounting medium, and fluorescence images were captured using a Leica DM5500 fluorescence microscope. $POMC^{ARH}$ neurons coexpressing SK3 were counted and averaged in at least five consecutive coronal brain slices containing the arcuate nucleus from each mouse. These data were treated as one biological sample, and statistical analyses were performed using data from three different mice.

Statistics

Statistical analyses were performed using GraphPad Prism 7.0 statistics software (San Diego, CA, USA). Statistical analysis methods were chosen based on the design of each experiment and indicated in the figure legends. The data were presented as mean ± SEM. $P \leq 0.05$ was considered statistically significant.

Supplementary Materials

This PDF file includes:

Figs. S1 to S13

REFERENCES AND NOTES

1. W. Luu, L. J. Sharpe, I. Capell-Hattam, I. C. Gelissen, A. J. Brown, Oxysterols: Old tale, new twists. *Annu. Rev. Pharmacol. Toxicol.* **56**, 447–467 (2016).

2. A. A. Kandutsch, H. W. Chen, H. J. Heiniger, Biological activity of some oxygenated sterols. *Science* **201**, 498–501 (1978).
3. S. Gill, R. Chow, A. J. Brown, Sterol regulators of cholesterol homeostasis and beyond: The oxysterol hypothesis revisited and revised. *Prog. Lipid Res.* **47**, 391–404 (2008).
4. A. A. Bielska, P. Schlesinger, D. F. Covey, D. S. Ory, Oxysterols as non-genomic regulators of cholesterol homeostasis. *Trends Endocrinol. Metab.* **23**, 99–106 (2012).
5. N. B. Javitt, 25R,26-Hydroxycholesterol revisited: Synthesis, metabolism, and biologic roles. *J. Lipid Res.* **43**, 665–670 (2002).
6. V. V. Bandaru, N. J. Haughey, Quantitative detection of free 24S-hydroxycholesterol, and 27-hydroxycholesterol from human serum. *BMC Neurosci.* **15**, 137 (2014).
7. D. Li, W. Long, R. Huang, Y. Chen, M. Xia, 27-Hydroxycholesterol inhibits sterol regulatory element-binding protein 1 activation and hepatic lipid accumulation in mice. *Obesity* **26**, 713–722 (2018).
8. L. P. Sun, J. Seemann, J. L. Goldstein, M. S. Brown, Sterol-regulated transport of SREBPs from endoplasmic reticulum to Golgi: Insig renders sorting signal in Scap inaccessible to COPII proteins. *Proc. Natl. Acad. Sci. U.S.A.* **104**, 6519–6526 (2007).
9. J. Westman, B. Kallin, I. Bjorkhem, J. Nilsson, U. Diczfalusy, Sterol 27-hydroxylase- and apoAI/phospholipid-mediated efflux of cholesterol from cholesterol-laden macrophages: Evidence for an inverse relation between the two mechanisms. *Arterioscler. Thromb. Vasc. Biol.* **18**, 554–561 (1998).
10. J. J. Bell, T. E. Sargeant, J. A. Watson, Inhibition of 3-hydroxy-3-methylglutaryl coenzyme A reductase activity in hepatoma tissue culture cells by pure cholesterol and several cholesterol derivatives. Evidence supporting two distinct mechanisms.20l. *J. Biol. Chem.* **251**, 1745–1758 (1976).
11. Y. Lange, D. S. Ory, J. Ye, M. H. Lanier, F. F. Hsu, T. L. Steck, Effectors of rapid homeostatic responses of endoplasmic reticulum cholesterol and 3-hydroxy-3-methylglutaryl-CoA reductase. *J. Biol. Chem.* **283**, 1445–1455 (2008).
12. F. R. Taylor, S. E. Saucier, E. P. Shown, E. J. Parish, A. A. Kandutsch, Correlation between oxysterol binding to a cytosolic binding protein and potency in the repression of hydroxymethylglutaryl coenzyme A reductase. *J. Biol. Chem.* **259**, 12382–12387 (1984).
13. E. Lund, O. Andersson, J. Zhang, A. Babiker, G. Ahlborg, U. Diczfalusy, K. Einarsson, J. Sjovall, I. Bjorkhem, Importance of a novel oxidative mechanism for elimination of intracellular cholesterol in humans. *Arterioscler. Thromb. Vasc. Biol.* **16**, 208–212 (1996).
14. U. Diczfalusy, E. Lund, D. Lutjohann, I. Bjorkhem, Novel pathways for elimination of cholesterol by extrahepatic formation of side-chain oxidized oxysterols. *Scand. J. Clin. Lab. Invest. Suppl.* **226**, 9–17 (1996).
15. A. Babiker, O. Andersson, D. Lindblom, J. van der Linden, B. Wiklund, D. Lutjohann, U. Diczfalusy, I. Bjorkhem, Elimination of cholesterol as cholestenoic acid in human lung by sterol 27-hydroxylase: Evidence that most of this steroid in the circulation is of pulmonary origin. *J. Lipid Res.* **40**, 1417–1425 (1999).
16. I. Bjorkhem, O. Andersson, U. Diczfalusy, B. Sevastik, R. J. Xiu, C. Duan, E. Lund, Atherosclerosis and sterol 27-hydroxylase: Evidence for a role of this enzyme in elimination of cholesterol from human macrophages. *Proc. Natl. Acad. Sci. U.S.A.* **91**, 8592–8596 (1994).
17. M. Umetani, P. W. Shaul, 27-Hydroxycholesterol: The first identified endogenous SERM. *Trends Endocrinol. Metab.* **22**, 130–135 (2011).
18. X. Fu, J. G. Menke, Y. Chen, G. Zhou, K. L. MacNaul, S. D. Wright, C. P. Sparrow, E. G. Lund, 27-Hydroxycholesterol is an endogenous ligand for liver X receptor in cholesterol-loaded cells. *J. Biol. Chem.* **276**, 38378–38387 (2001).
19. I. G. Schulman, Liver X receptors link lipid metabolism and inflammation. *FEBS Lett.* **591**, 2978–2991 (2017).
20. S. He, E. R. Nelson, 27-Hydroxycholesterol, an endogenous selective estrogen receptor modulator. *Maturitas* **104**, 29–35 (2017).
21. M. Umetani, H. Domoto, A. K. Gormley, I. S. Yuhanna, C. L. Cummins, N. B. Javitt, K. S. Korach, P. W. Shaul, D. J. Mangelsdorf, 27-Hydroxycholesterol is an endogenous SERM that inhibits the cardiovascular effects of estrogen. *Nat. Med.* **13**, 1185–1192 (2007).
22. M. Umetani, P. Ghosh, T. Ishikawa, J. Umetani, M. Ahmed, C. Mineo, P. W. Shaul, The cholesterol metabolite 27-hydroxycholesterol promotes atherosclerosis via proinflammatory processes mediated by estrogen receptor alpha. *Cell Metab.* **20**, 172–182 (2014).
23. M. Hilsch, I. Haralampiev, P. Muller, D. Huster, H. A. Scheidt, Membrane properties of hydroxycholesterols related to the brain cholesterol metabolism. *Beilstein J. Org. Chem.* **13**, 720–727 (2017).
24. M. Heverin, S. Meaney, D. Lütjohann, U. Diczfalusy, J. Wahren, I. Björkhem, Crossing the barrier: Net flux of 27-hydroxycholesterol into the human brain. *J. Lipid Res.* **46**, 1047–1052 (2005).
25. V. Leoni, T. Masterman, F. S. Mousavi, B. Wretlind, L. O. Wahlund, U. Diczfalusy, J. Hillert, I. Bjorkhem, Diagnostic use of cerebral and extracerebral oxysterols. *Clin. Chem. Lab. Med.* **42**, 186–191 (2004).
26. S. W. Brooks, A. C. Dykes, B. G. Schreurs, A high-cholesterol diet increases 27-hydroxycholesterol and modifies estrogen receptor expression and neurodegeneration in rabbit hippocampus. *J. Alzheimers Dis.* **56**, 185–196 (2017).
27. V. Leoni, T. Masterman, P. Patel, S. Meaney, U. Diczfalusy, I. Björkhem, Side chain oxidized oxysterols in cerebrospinal fluid and the integrity of blood-brain and blood-cerebrospinal fluid barriers. *J. Lipid Res.* **44**, 793–799 (2003).
28. H. L. Wang, Y. Y. Wang, X. G. Liu, S. H. Kuo, N. Liu, Q. Y. Song, M. W. Wang, Cholesterol, 24-hydroxycholesterol, and 27-hydroxycholesterol as surrogate biomarkers in cerebrospinal fluid in mild cognitive impairment and Alzheimer's disease: A meta-analysis. *J. Alzheimers Dis.* **51**, 45–55 (2016).
29. G. Testa, E. Staurenghi, C. Zerbinati, S. Gargiulo, L. Iuliano, G. Giaccone, F. Fanto, G. Poli, G. Leonarduzzi, P. Gamba, Changes in brain oxysterols at different stages of Alzheimer's disease: Their involvement in neuroinflammation. *Redox Biol.* **10**, 24–33 (2016).
30. J. Popp, P. Lewczuk, H. Kolsch, S. Meichsner, W. Maier, J. Kornhuber, F. Jessen, D. Lutjohann, Cholesterol metabolism is associated with soluble amyloid precursor protein production in Alzheimer's disease. *J. Neurochem.* **123**, 310–316 (2012).
31. P. Xu, X. Cao, Y. Xu, Targeting brain estrogen receptor for binge eating. *Oncotarget* **6**, 23044–23045 (2015).
32. Y. Xu, M. Lopez, Central regulation of energy metabolism by estrogens. *Mol. Metab.* **15**, 104–115 (2018).
33. V. C. Torres Irizarry, Y. Jiang, Y. He, P. Xu, Hypothalamic estrogen signaling and adipose tissue metabolism in energy homeostasis. *Front. Endocrinol.* **13**, 898139 (2022).
34. Y. He, P. Xu, X. Yan, Y. Yang, X. Cai, I. Hyseni, X. Yong, Estrogen-responsive neurons in the ventrolateral VMH regulate glucose balance. *Diabetes* **67**, 2165 (2018).
35. Y. He, P. Xu, C. Wang, Y. Xia, M. Yu, Y. Yang, K. Yu, X. Cai, N. Qu, K. Saito, J. Wang, I. Hyseni, M. Robertson, B. Piyarathna, M. Gao, S. A. Khan, F. Liu, R. Chen, C. Coarfa, Z. Zhao, Q. Tong, Z. Sun, Y. Xu, Estrogen receptor-α expressing neurons in the ventrolateral VMH regulate glucose balance. *Nat. Commun.* **11**, 2165 (2020).
36. M. H. Oosterveer, A. Grefhorst, A. K. Groen, F. Kuipers, The liver X receptor: Control of cellular lipid homeostasis and beyond implications for drug design. *Prog. Lipid Res.* **49**, 343–352 (2010).
37. L. Wang, G. U. Schuster, K. Hultenby, Q. Zhang, S. Andersson, J. A. Gustafsson, Liver X receptors in the central nervous system: From lipid homeostasis to neuronal degeneration. *Proc. Natl. Acad. Sci. U.S.A.* **99**, 13878–13883 (2002).
38. R. Courtney, G. E. Landreth, LXR regulation of brain cholesterol: From development to disease. *Trends Endocrinol. Metab.* **27**, 404–414 (2016).
39. J. J. Repa, H. Li, T. C. Frank-Cannon, M. A. Valasek, S. D. Turley, M. G. Tansey, J. M. Dietschy, Liver X receptor activation enhances cholesterol loss from the brain, decreases neuroinflammation, and increases survival of the NPC1 mouse. *J. Neurosci.* **27**, 14470–14480 (2007).
40. D. D. Zhang, H. L. Yu, W. W. Ma, Q. R. Liu, J. Han, H. Wang, R. Xiao, 27-Hydroxycholesterol contributes to disruptive effects on learning and memory by modulating cholesterol metabolism in the rat brain. *Neuroscience* **300**, 163–173 (2015).
41. J. Liu, K. Jiao, Q. Zhou, J. Yang, K. Yang, C. Hu, M. Zhou, Z. Li, Resveratrol alleviates 27-hydroxycholesterol-induced senescence in nerve cells and affects zebrafish locomotor behavior via activation of SIRT1-mediated STAT3 signaling. *Oxid. Med. Cell. Longev.* **2021**, 6673343 (2021).
42. R. Loera-Valencia, M. A. Ismail, J. Goikolea, M. Lodeiro, L. Mateos, I. Bjorkhem, E. Puerta, M. A. Romao, C. M. Gomes, P. Merino-Serrais, S. Maioli, A. Cedazo-Minguez, Hypercholesterolemia and 27-hydroxycholesterol increase S100A8 and RAGE expression in the brain: A link between cholesterol, alarmins, and neurodegeneration. *Mol. Neurobiol.* **58**, 6063–6076 (2021).
43. W. W. Ma, C. Q. Li, L. Zhao, Y. S. Wang, R. Xiao, NF-κB-mediated inflammatory damage is differentially affected in SH-SY5Y and C6 cells treated with 27-hydroxycholesterol. *Food Sci. Nutr.* **7**, 1685–1694 (2019).
44. J. Liu, Y. Liu, J. Chen, C. Hu, M. Teng, K. Jiao, Z. Shen, D. Zhu, J. Yue, Z. Li, Y. Li, The ROS-mediated activation of IL-6/STAT3 signaling pathway is involved in the 27-hydroxycholesterol-induced cellular senescence in nerve cells. *Toxicol. In Vitro* **45**, 10–18 (2017).
45. M. A. Ismail, L. Mateos, S. Maioli, P. Merino-Serrais, Z. Ali, M. Lodeiro, E. Westman, E. Leitersdorf, B. Gulyas, L. Olof-Wahlund, B. Winblad, I. Savitcheva, I. Bjorkhem, A. Cedazo-Minguez, 27-Hydroxycholesterol impairs neuronal glucose uptake through an IRAP/GLUT4 system dysregulation. *J. Exp. Med.* **214**, 699–717 (2017).
46. A. Asghari, T. Ishikawa, S. Hiramitsu, W. R. Lee, J. Umetani, L. Bui, K. S. Korach, M. Umetani, 27-Hydroxycholesterol promotes adiposity and mimics adipogenic diet-induced inflammatory signaling. *Endocrinology* **160**, 2485–2494 (2019).
47. S. A. McClave, C. C. Lowen, M. J. Kleber, J. W. McConnell, L. Y. Jung, L. J. Goldsmith, Clinical use of the respiratory quotient obtained from indirect calorimetry. *J. Parenter. Enteral Nutr.* **27**, 21–26 (2003).
48. K. N. Frayn, Calculation of substrate oxidation rates in vivo from gaseous exchange. *J. Appl. Physiol. Respir. Environ. Exerc. Physiol.* **55**, 628–634 (1983).
49. R. E. Patterson, D. D. Sears, Metabolic effects of intermittent fasting. *Annu. Rev. Nutr.* **37**, 371–393 (2017).

50. K. Saito, Y. He, X. Yan, Y. Yang, C. Wang, P. Xu, A. O. Hinton Jr., G. Shu, L. Yu, Q. Tong, Y. Xu, Visualizing estrogen receptor-α-expressing neurons using a new ERα-ZsGreen reporter mouse line. *Metabolism* **65**, 522–532 (2016).
51. J. Cao, H. B. Patisaul, Sexually dimorphic expression of hypothalamic estrogen receptors α and β and Kiss1 in neonatal male and female rats. *J. Comp. Neurol.* **519**, 2954–2977 (2011).
52. Y. Xu, T. P. Nedungadi, L. Zhu, N. Sobhani, B. G. Irani, K. E. Davis, X. Zhang, F. Zou, L. M. Gent, L. D. Hahner, S. A. Khan, C. F. Elias, J. K. Elmquist, D. J. Clegg, Distinct hypothalamic neurons mediate estrogenic effects on energy homeostasis and reproduction. *Cell Metab.* **14**, 453–465 (2011).
53. F. E. Henry, K. Sugino, A. Tozer, T. Branco, S. M. Sternson, Cell type-specific transcriptomics of hypothalamic energy-sensing neuron responses to weight-loss. *eLife* **4**, (2015).
54. I. Mishra, W. R. Xie, J. C. Bournat, Y. He, C. Wang, E. S. Silva, H. Liu, Z. Ku, Y. Chen, B. O. Erokwu, P. Jia, Z. Zhao, Z. An, C. A. Flask, Y. He, Y. Xu, A. R. Chopra, Protein tyrosine phosphatase receptor δ serves as the orexigenic asprosin receptor. *Cell Metab.* **34**, 549–563.e8 (2022).
55. B. Feng, H. Liu, I. Mishra, C. Duerrschmid, P. Gao, P. Xu, C. Wang, Y. He, Asprosin promotes feeding through SK channel-dependent activation of AgRP neurons. *Sci. Adv.* **9**, eabq6718 (2023).
56. G. W. Millington, The role of proopiomelanocortin (POMC) neurones in feeding behaviour. *Nutr. Metab.* **4**, 18 (2007).
57. O. P. Soldin, D. R. Mattison, Sex differences in pharmacokinetics and pharmacodynamics. *Clin. Pharmacokinet.* **48**, 143–157 (2009).
58. A. Horstmann, P. Kovacs, S. Kabisch, Y. Boettcher, H. Schloegl, A. Tonjes, M. Stumvoll, B. Pleger, A. Villringer, Common genetic variation near MC4R has a sex-specific impact on human brain structure and eating behavior. *PLOS ONE* **8**, e74362 (2013).
59. R. N. Lippert, K. L. Ellacott, R. D. Cone, Gender-specific roles for the melanocortin-3 receptor in the regulation of the mesolimbic dopamine system in mice. *Endocrinology* **155**, 1718–1727 (2014).
60. P. C. Butera, Estradiol and the control of food intake. *Physiol. Behav.* **99**, 175–180 (2010).
61. S. Thammacharoen, T. A. Lutz, N. Geary, L. Asarian, Hindbrain administration of estradiol inhibits feeding and activates estrogen receptor-alpha-expressing cells in the nucleus tractus solitarius of ovariectomized rats. *Endocrinology* **149**, 1609–1617 (2008).
62. L. Shen, Y. Liu, D. Q. Wang, P. Tso, S. C. Woods, M. Liu, Estradiol stimulates apolipoprotein A-IV gene expression in the nucleus of the solitary tract through estrogen receptor-α. *Endocrinology* **155**, 3882–3890 (2014).
63. A. G. Uner, O. Kecik, P. G. F. Quaresma, T. M. De Araujo, H. Lee, W. Li, H. J. Kim, M. Chung, C. Bjorbaek, Y. B. Kim, Role of POMC and AgRP neuronal activities on glycaemia in mice. *Sci. Rep.* **9**, 13068 (2019).
64. M. Yu, J. C. Bean, H. Liu, Y. He, Y. Yang, X. Cai, K. Yu, Z. Pei, H. Liu, L. Tu, K. M. Conde, M. Wang, Y. Li, N. Yin, N. Zhang, J. Han, N. A. Scarcelli, P. Xu, Y. He, Y. Xu, C. Wang, SK3 in POMC neurons plays a sexually dimorphic role in energy and glucose homeostasis. *Cell Biosci.* **12**, 170 (2022).
65. X. Cao, P. Xu, M. G. Oyola, Y. Xia, X. Yan, K. Saito, F. Zou, C. Wang, Y. Yang, A. Hinton Jr., C. Yan, H. Ding, L. Zhu, L. Yu, B. Yang, Y. Feng, D. J. Clegg, S. Khan, R. DiMarchi, S. K. Mani, Q. Tong, Y. Xu, Estrogens stimulate serotonin neurons to inhibit binge-like eating in mice. *J. Clin. Invest.* **124**, 4351–4362 (2014).
66. J. Sun, Y. Liu, M. Baudry, X. Bi, SK2 channel regulation of neuronal excitability, synaptic transmission, and brain rhythmic activity in health and diseases. *Biochim. Biophys. Acta Mol. Cell. Res.* **1867**, 118834 (2020).
67. J. P. Adelman, J. Maylie, P. Sah, Small-conductance Ca^{2+}–activated K^+ channels: Form and function. *Annu. Rev. Physiol.* **74**, 245–269 (2012).
68. M. Kohler, B. Hirschberg, C. T. Bond, J. M. Kinzie, N. V. Marrion, J. Maylie, J. P. Adelman, Small-conductance, calcium-activated potassium channels from mammalian brain. *Science* **273**, 1709–1714 (1996).
69. M. Stocker, P. Pedarzani, Differential distribution of three Ca^{2+}-activated K^+ channel subunits, SK1, SK2, and SK3, in the adult rat central nervous system. *Mol. Cell. Neurosci.* **15**, 476–493 (2000).
70. J. Popp, S. Meichsner, H. Kolsch, P. Lewczuk, W. Maier, J. Kornhuber, F. Jessen, D. Lutjohann, Cerebral and extracerebral cholesterol metabolism and CSF markers of Alzheimer's disease. *Biochem. Pharmacol.* **86**, 37–42 (2013).
71. L. Novakova, M. Axelsson, C. Malmestrom, H. Zetterberg, I. Bjorkhem, V. D. Karrenbauer, J. Lycke, Reduced cerebrospinal fluid concentrations of oxysterols in response to natalizumab treatment of relapsing remitting multiple sclerosis. *J. Neurol. Sci.* **358**, 201–206 (2015).
72. M. Shafaati, A. Solomon, M. Kivipelto, I. Bjorkhem, V. Leoni, Levels of ApoE in cerebrospinal fluid are correlated with Tau and 24S-hydroxycholesterol in patients with cognitive disorders. *Neurosci. Lett.* **425**, 78–82 (2007).
73. R. Karuna, A. G. Holleboom, M. M. Motazacker, J. A. Kuivenhoven, R. Frikke-Schmidt, A. Tybjaerg-Hansen, S. Georgopoulos, M. van Eck, T. J. van Berkel, A. von Eckardstein, K. M. Rentsch, Plasma levels of 27-hydroxycholesterol in humans and mice with monogenic disturbances of high density lipoprotein metabolism. *Atherosclerosis* **214**, 448–455 (2011).
74. E. R. Nelson, C. D. DuSell, X. Wang, M. K. Howe, G. Evans, R. D. Michalek, M. Umetani, J. C. Rathmell, S. Khosla, D. Gesty-Palmer, D. P. McDonnell, The oxysterol, 27-hydroxycholesterol, links cholesterol metabolism to bone homeostasis through its actions on the estrogen and liver X receptors. *Endocrinology* **152**, 4691–4705 (2011).
75. C. Parrado-Fernandez, V. Leoni, A. Saeed, P. Rodriguez-Rodriguez, A. Sandebring-Matton, C. M. Cordoba-Beldad, P. Bueno, C. C. Gali, U. Panzenboeck, A. Cedazo-Minguez, I. Bjorkhem, Sex difference in flux of 27-hydroxycholesterol into the brain. *Br. J. Pharmacol.* **178**, 3194–3204 (2021).
76. A. R. Stiles, J. G. McDonald, D. R. Bauman, D. W. Russell, CYP7B1: One cytochrome P450, two human genetic diseases, and multiple physiological functions. *J. Biol. Chem.* **284**, 28485–28489 (2009).
77. S. Nie, G. Chen, X. Cao, Y. Zhang, Cerebrotendinous xanthomatosis: A comprehensive review of pathogenesis, clinical manifestations, diagnosis, and management. *Orphanet J. Rare Dis.* **9**, 179 (2014).
78. K. Meir, D. Kitsberg, I. Alkalay, F. Szafer, H. Rosen, S. Shpitzen, L. B. Avi, B. Staels, C. Fievet, V. Meiner, I. Bjorkhem, E. Leitersdorf, Human sterol 27-hydroxylase (CYP27) overexpressor transgenic mouse model. *J. Biol. Chem.* **277**, 34036–34041 (2002).
79. R. Loera-Valencia, E. Vazquez-Juarez, A. Muñoz, G. Gerenu, M. Gómez-Galán, M. Lindskog, J. DeFelipe, A. Cedazo-Minguez, P. Merino-Serrais, High levels of 27-hydroxycholesterol results in synaptic plasticity alterations in the hippocampus. *Sci. Rep.* **11**, 3736 (2021).
80. P. Merino-Serrais, R. Loera-Valencia, P. Rodriguez-Rodriguez, C. Parrado-Fernandez, M. A. Ismail, S. Maioli, E. Matute, E. M. Jimenez-Mateos, I. Björkhem, J. DeFelipe, 27-Hydroxycholesterol induces aberrant morphology and synaptic dysfunction in hippocampal neurons. *Cereb. Cortex* **29**, 429–446 (2019).
81. P. Gamba, E. Staurenghi, G. Testa, S. Giannelli, B. Sottero, G. Leonarduzzi, A crosstalk between brain cholesterol oxidation and glucose metabolism in Alzheimer's disease. *Front. Neurosci.* **13**, 556 (2019).
82. I. Y. Kim, S. Park, J. Jang, R. R. Wolfe, Quantifications of lipid kinetics in vivo using stable isotope tracer methodology. *J. Lipid Atheroscler.* **9**, 110–123 (2020).
83. I. Y. Kim, S. H. Suh, I. K. Lee, R. R. Wolfe, Applications of stable, nonradioactive isotope tracers in in vivo human metabolic research. *Exp. Mol. Med.* **48**, e203 (2016).
84. J. M. Lehmann, S. A. Kliewer, L. B. Moore, T. A. Smith-Oliver, B. B. Oliver, J. L. Su, S. S. Sundseth, D. A. Winegar, D. E. Blanchard, T. A. Spencer, T. M. Willson, Activation of the nuclear receptor LXR by oxysterols defines a new hormone response pathway. *J. Biol. Chem.* **272**, 3137–3140 (1997).
85. M. Faouzi, R. Leshan, M. Bjornholm, T. Hennessey, J. Jones, H. Munzberg, Differential accessibility of circulating leptin to individual hypothalamic sites. *Endocrinology* **148**, 5414–5423 (2007).
86. E. M. Rodriguez, J. L. Blazquez, M. Guerra, The design of barriers in the hypothalamus allows the median eminence and the arcuate nucleus to enjoy private milieus: The former opens to the portal blood and the latter to the cerebrospinal fluid. *Peptides* **31**, 757–776 (2010).
87. L. Harrison, S. C. Schriever, A. Feuchtinger, E. Kyriakou, P. Baumann, K. Pfuhlmann, A. C. Messias, A. Walch, M. H. Tschop, P. T. Pfluger, Fluorescent blood-brain barrier tracing shows intact leptin transport in obese mice. *Int. J. Obes. (Lond)* **43**, 1305–1318 (2019).
88. N. Romano, C. Lafont, P. Campos, A. Guillou, T. Fiordelisio, D. J. Hodson, P. Mollard, M. Schaeffer, Median eminence blood flow influences food intake by regulating ghrelin access to the metabolic brain. *JCI Insight* **8**, e165763 (2023).
89. G. Stapleton, M. Steel, M. Richardson, J. O. Mason, K. A. Rose, R. G. Morris, R. Lathe, A novel cytochrome P450 expressed primarily in brain. *J. Biol. Chem.* **270**, 29739–29745 (1995).
90. M. J. Simon, J. J. Iliff, Regulation of cerebrospinal fluid (CSF) flow in neurodegenerative, neurovascular and neuroinflammatory disease. *Biochim. Biophys. Acta* **1862**, 442–451 (2016).
91. S. L. Padilla, D. Reef, L. M. Zeltser, Defining POMC neurons using transgenic reagents: Impact of transient Pomc expression in diverse immature neuronal populations. *Endocrinology* **153**, 1219–1231 (2012).
92. W. C. Krause, R. Rodriguez, B. Gegenhuber, N. Matharu, A. N. Rodriguez, A. M. Padilla-Roger, K. Toma, C. B. Herber, S. M. Correa, X. Duan, N. Ahituv, J. Tollkuhn, H. A. Ingraham, Oestrogen engages brain MC4R signalling to drive physical activity in female mice. *Nature* **599**, 131–135 (2021).
93. S. E. Alves, V. Lopez, B. S. McEwen, N. G. Weiland, Differential colocalization of estrogen receptor beta (ERbeta) with oxytocin and vasopressin in the paraventricular and supraoptic nuclei of the female rat brain: An immunocytochemical study. *Proc. Natl. Acad. Sci. U.S.A.* **95**, 3281–3286 (1998).
94. B. Greco, E. A. Allegretto, M. J. Tetel, J. D. Blaustein, Coexpression of ER beta with ER alpha and progestin receptor proteins in the female rat forebrain: Effects of estradiol treatment. *Endocrinology* **142**, 5172–5181 (2001).
95. P. Xu, X. Cao, Y. He, L. Zhu, Y. Yang, K. Saito, C. Wang, X. Yan, A. O. Hinton Jr., F. Zou, H. Ding, Y. Xia, C. Yan, G. Shu, S. P. Wu, B. Yang, Y. Feng, D. J. Clegg, R. DeMarchi, S. A. Khan, S. Y. Tsai, F. J. DeMayo, Q. Wu, Q. Tong, Y. Xu, Estrogen receptor–α in medial amygdala neurons regulates body weight. *J. Clin. Invest.* **125**, 2861–2876 (2015).
96. C. A. Campos, A. J. Bowen, M. W. Schwartz, R. D. Palmiter, Parabrachial CGRP neurons control meal termination. *Cell Metab.* **23**, 811–820 (2016).

97. D. Mishra, J. E. Richard, I. Maric, B. Porteiro, M. Haring, S. Kooijman, S. Musovic, K. Eerola, L. Lopez-Ferreras, E. Peris, K. Grycel, O. T. Shevchouk, P. Micallef, C. S. Olofsson, I. Wernstedt Asterholm, H. J. Grill, R. Nogueiras, K. P. Skibicka, Parabrachial interleukin-6 reduces body weight and food intake and increases thermogenesis to regulate energy metabolism. *Cell Rep.* **26**, 3011–3026.e5 (2019).
98. J. Jordi, B. Herzog, S. M. Camargo, C. N. Boyle, T. A. Lutz, F. Verrey, Specific amino acids inhibit food intake via the area postrema or vagal afferents. *J. Physiol.* **591**, 5611–5621 (2013).
99. V. G. Vanderhorst, E. Terasawa, H. J. Ralston III, Estrogen receptor-alpha immunoreactive neurons in the brainstem and spinal cord of the female rhesus monkey: Species-specific characteristics. *Neuroscience* **158**, 798–810 (2009).
100. P. V. Sabatini, H. Frikke-Schmidt, J. Arthurs, D. Gordian, A. Patel, A. C. Rupp, J. M. Adams, J. Wang, S. Beck Jorgensen, D. P. Olson, R. D. Palmiter, M. G. Myers Jr., R. J. Seeley, GFRAL-expressing neurons suppress food intake via aversive pathways. *Proc. Natl. Acad. Sci. U.S.A.* **118**, e2021357118 (2021).
101. S. E. Kanoski, H. J. Grill, Hippocampus contributions to food intake control: Mnemonic, neuroanatomical, and endocrine mechanisms. *Biol. Psychiatry* **81**, 748–756 (2017).
102. T. M. Hsu, J. D. Hahn, V. R. Konanur, E. E. Noble, A. N. Suarez, J. Thai, E. M. Nakamoto, S. E. Kanoski, Hippocampus ghrelin signaling mediates appetite through lateral hypothalamic orexin pathways. *eLife* **4**, (2015).
103. J. Santollo, A. Marshall, D. Daniels, Activation of membrane-associated estrogen receptors decreases food and water intake in ovariectomized rats. *Endocrinology* **154**, 320–329 (2013).
104. T. P. Donohoe, R. Stevens, Modulation of food intake by hypothalamic implants of estradiol benzoate, estrone, estriol and CI-628 in female rats. *Pharmacol. Biochem. Behav.* **16**, 93–99 (1982).
105. Z. Zhang, F. Reis, Y. He, J. W. Park, J. R. DiVittorio, N. Sivakumar, J. E. van Veen, S. Maesta-Pereira, M. Shum, I. Nichols, M. G. Massa, S. Anderson, K. Paul, M. Liesa, O. A. Ajijola, Y. Xu, A. Adhikari, S. M. Correa, Estrogen-sensitive medial preoptic area neurons coordinate torpor in mice. *Nat. Commun.* **11**, 6378 (2020).
106. K. Yu, Y. He, I. Hyseni, Z. Pei, Y. Yang, P. Xu, X. Cai, H. Liu, N. Qu, H. Liu, Y. He, M. Yu, C. Liang, T. Yang, J. Wang, P. Gourdy, J. F. Arnal, F. Lenfant, Y. Xu, C. Wang, 17β-Estradiol promotes acute refeeding in hungry mice via membrane-initiated ERα signaling. *Mol. Metab.* **42**, 101053 (2020).
107. C. Zhan, J. Zhou, Q. Feng, J.-E. Zhang, S. Lin, J. Bao, P. Wu, M. Luo, Acute and long-term suppression of feeding behavior by POMC neurons in the brainstem and hypothalamus, respectively. *J. Neurosci.* **33**, 3624–3632 (2013).
108. Y. Aponte, D. Atasoy, S. M. Sternson, AGRP neurons are sufficient to orchestrate feeding behavior rapidly and without training. *Nat. Neurosci.* **14**, 351–355 (2011).
109. J. N. Campbell, E. Z. Macosko, H. Fenselau, T. H. Pers, A. Lyubetskaya, D. Tenen, M. Goldman, A. M. Verstegen, J. M. Resch, S. A. McCarroll, E. D. Rosen, B. B. Lowell, L. T. Tsai, A molecular census of arcuate hypothalamus and median eminence cell types. *Nat. Neurosci.* **20**, 484–496 (2017).
110. N. Biglari, I. Gaziano, J. Schumacher, J. Radermacher, L. Paeger, P. Klemm, W. Chen, S. Corneliussen, C. M. Wunderlich, M. Sue, S. Vollmar, T. Klockener, T. Sotelo-Hitschfeld, A. Abbasloo, F. Edenhofer, F. Reimann, F. M. Gribble, H. Fenselau, P. Kloppenburg, F. T. Wunderlich, J. C. Bruning, Functionally distinct POMC-expressing neuron subpopulations in hypothalamus revealed by intersectional targeting. *Nat. Neurosci.* **24**, 913–929 (2021).
111. M. Koch, L. Varela, J. G. Kim, J. D. Kim, F. Hernandez-Nuno, S. E. Simonds, C. M. Castorena, C. R. Vianna, J. K. Elmquist, Y. M. Morozov, P. Rakic, I. Bechmann, M. A. Cowley, K. Szigeti-Buck, M. O. Dietrich, X. B. Gao, S. Diano, T. L. Horvath, Hypothalamic POMC neurons promote cannabinoid-induced feeding. *Nature* **519**, 45–50 (2015).
112. Q. Wei, D. M. Krolewski, S. Moore, V. Kumar, F. Li, B. Martin, R. Tomer, G. G. Murphy, K. Deisseroth, S. J. Watson Jr., H. Akil, Uneven balance of power between hypothalamic peptidergic neurons in the control of feeding. *Proc. Natl. Acad. Sci. U.S.A.* **115**, E9489–E9498 (2018).
113. E. R. Nelson, S. E. Wardell, J. S. Jasper, S. Park, S. Suchindran, M. K. Howe, N. J. Carver, R. V. Pillai, P. M. Sullivan, V. Sondhi, M. Umetani, J. Geradts, D. P. McDonnell, 27-Hydroxycholesterol links hypercholesterolemia and breast cancer pathophysiology. *Science* **342**, 1094–1098 (2013).
114. Q. Wu, T. Ishikawa, R. Sirianni, H. Tang, J. G. McDonald, I. S. Yuhanna, B. Thompson, L. Girard, C. Mineo, R. A. Brekken, M. Umetani, D. M. Euhus, Y. Xie, P. W. Shaul, 27-Hydroxycholesterol promotes cell-autonomous, ER-positive breast cancer growth. *Cell Rep.* **5**, 637–645 (2013).
115. I. Shagufta, Tamoxifen a pioneering drug: An update on the therapeutic potential of tamoxifen derivatives. *Eur. J. Med. Chem.* **143**, 515–531 (2018).
116. G. N. Wade, H. W. Heller, Tamoxifen mimics the effects of estradiol on food intake, body weight, and body composition in rats. *Am. J. Physiol.* **264**, R1219–R1223 (1993).
117. C. Wang, Y. He, P. Xu, Y. Yang, K. Saito, Y. Xia, X. Yan, A. Hinton Jr., C. Yan, H. Ding, L. Yu, G. Shu, R. Gupta, Q. Wu, Q. Tong, W. R. Lagor, E. R. Flores, Y. Xu, TAp63 contributes to sexual dimorphism in POMC neuron functions and energy homeostasis. *Nat. Commun.* **9**, 1544 (2018).
118. X. Liu, H. Shi, Regulation of estrogen receptor α expression in the hypothalamus by sex steroids: Implication in the regulation of energy homeostasis. *Int. J. Endocrinol.* **2015**, 949085 (2015).
119. K. A. Rose, G. Stapleton, K. Dott, M. P. Kieny, R. Best, M. Schwarz, D. W. Russell, I. Bjorkhem, J. Seckl, R. Lathe, Cyp7b, a novel brain cytochrome P450, catalyzes the synthesis of neurosteroids 7alpha-hydroxy dehydroepiandrosterone and 7alpha-hydroxy pregnenolone. *Proc. Natl. Acad. Sci. U.S.A.* **94**, 4925–4930 (1997).
120. K. Rose, A. Allan, S. Gauldie, G. Stapleton, L. Dobbie, K. Dott, C. Martin, L. Wang, E. Hedlund, J. R. Seckl, J. A. Gustafsson, R. Lathe, Neurosteroid hydroxylase CYP7B. *J. Biol. Chem.* **276**, 23937–23944 (2001).
121. W. Tang, M. Norlin, Regulation of steroid hydroxylase CYP7B1 by androgens and estrogens in prostate cancer LNCaP cells. *Biochem. Biophys. Res. Commun.* **344**, 540–546 (2006).
122. W. Tang, G. Eggertsen, J. Y. Chiang, M. Norlin, Estrogen-mediated regulation of CYP7B1: A possible role for controlling DHEA levels in human tissues. *J. Steroid Biochem. Mol. Biol.* **100**, 42–51 (2006).
123. Y. Feng, D. Manka, K.-U. Wagner, S. A. Khan, Estrogen receptor-α expression in the mammary epithelium is required for ductal and alveolar morphogenesis in mice. *Proc. Natl. Acad. Sci. U.S.A.* **104**, 14718–14723 (2007).
124. L. Zhu, P. Xu, X. Cao, Y. Yang, A. O. Hinton Jr., Y. Xia, K. Saito, X. Yan, F. Zou, H. Ding, C. Wang, C. Yan, P. Saha, S. A. Khan, J. Zhao, M. Fukuda, Q. Tong, D. J. Clegg, L. Chan, Y. Xu, The ERα-PI3K cascade in proopiomelanocortin progenitor neurons regulates feeding and glucose balance in female mice. *Endocrinology* **156**, 4474–4491 (2015).
125. C. Zhu, P. Xu, Y. He, Y. Yuan, T. Wang, X. Cai, L. Yu, L. Yang, J. Wu, L. Wang, X. Zhu, S. Wang, P. Gao, Q. Xi, Y. Zhang, Y. Xu, Q. Jiang, G. Shu, Heparin increases food intake through AgRP neurons. *Cell Rep.* **20**, 2455–2467 (2017).
126. H. Ye, B. Feng, C. Wang, K. Saito, Y. Yang, L. Ibrahimi, S. Schaul, N. Patel, L. Saenz, P. Luo, P. Lai, V. Torres, M. Kota, D. Dixit, X. Cai, N. Qu, I. Hyseni, K. Yu, Y. Jiang, Q. Tong, Z. Sun, B. R. Arenkiel, Y. He, P. Xu, Y. Xu, An estrogen-sensitive hypothalamus-midbrain neural circuit controls thermogenesis and physical activity. *Sci. Adv.* **8**, eabk0185 (2022).
127. A. I. Mina, R. A. LeClair, K. B. LeClair, D. E. Cohen, L. Lantier, A. S. Banks, CalR: A web-based analysis tool for indirect calorimetry experiments. *Cell Metab.* **28**, 656–666.e1 (2018).
128. Z. Pei, Y. He, J. C. Bean, Y. Yang, H. Liu, M. Yu, K. Yu, I. Hyseni, X. Cai, H. Liu, N. Qu, L. Tu, K. M. Conde, M. Wang, Y. Li, N. Yin, N. Zhang, J. Han, C. H. Potts, N. A. Scarcelli, Z. Yan, P. Xu, Q. Wu, Y. He, Y. Xu, C. Wang, Gabra5 plays a sexually dimorphic role in POMC neuron activity and glucose balance. *Front. Endocrinol.* **13**, 889122 (2022).
129. D. Mashiko, S. A. Young, M. Muto, H. Kato, K. Nozawa, M. Ogawa, T. Noda, Y. J. Kim, Y. Satouh, Y. Fujihara, M. Ikawa, Feasibility for a large scale mouse mutagenesis by injecting CRISPR/Cas plasmid into zygotes. *Dev. Growth Differ.* **56**, 122–129 (2014).
130. M. S. Gold, M. J. Shuster, J. D. Levine, Role of a Ca^{2+}-dependent slow afterhyperpolarization in prostaglandin E2-induced sensitization of cultured rat sensory neurons. *Neurosci. Lett.* **205**, 161–164 (1996).
131. P. Pagadala, C. K. Park, S. Bang, Z. Z. Xu, R. G. Xie, T. Liu, B. X. Han, W. D. Tracey Jr., F. Wang, R. R. Ji, Loss of NR1 subunit of NMDARs in primary sensory neurons leads to hyperexcitability and pain hypersensitivity: Involvement of Ca^{2+}-activated small conductance potassium channels. *J. Neurosci.* **33**, 13425–13430 (2013).
132. Y. He, G. Shu, Y. Yang, P. Xu, Y. Xia, C. Wang, K. Saito, A. Hinton Jr., X. Yan, C. Liu, Q. Wu, Q. Tong, Y. Xu, A small potassium current in AgRP/NPY neurons regulates feeding behavior and energy metabolism. *Cell Rep.* **17**, 1807–1818 (2016).

Acknowledgments: We wish to thank the Laboratory of Animal Center of Pennington Biomedical Research Center at Louisiana State University, Baylor College of Medicine, and The University of Illinois at Chicago for invaluable help in mouse colony maintenance. **Funding:** This work was supported by grants from National Research Foundation Singapore under its Young Individual Research Grant (OFYIRG-MOH-001515 to H.Y.) and administered by the Singapore Ministry of Health's National Medical Research Council; Singapore MOE AcRF Tier 1 (RG90/23) to H.Y.; NTU-Research Scholarship R2301921 to X.Q.; NIH (R01 DK123098 and P30 DK020595 to P.X.; P20 GM135002 and R01 DK129548 to Y.H.; R01 DK132398 to Y.J.; R01 DK109015 and P30 DK020595 to C.W.L.; T32 AA026577 and F31 DK132918 to V.C.T.I.; K01 DK119471 and R01 DK136627 to C.W.); USDA/CRIS [3092-1000-062-04(B)S to C.W.]; AHA (2021AHA000PRE0000215743 to V.C.T.I.; 19CDA34660335 to C.W.; 20POST35120600 to Y.H.); and DOD (Innovative Grant W81XWH-20-1-0075 to P.X.). **Author contributions:** H.Y. and X.Y. are the main contributors to the conduct of the study, data collection and analysis, data interpretation, and manuscript writing. B.F., P.Lu., V.C.T.I., L.C.-S., M.Y., Y.Y., B.P.E., M.D.M., N.P., S.S., L.I., P.La., X.Q., Y.Z., M.K., D.D., and M.M. contributed to the conduct of the study. C.W.L., Y.J., C.W., Y.H., and P.X. contributed to the study design, data interpretation, and manuscript writing. **Competing interests:** The authors declare that they have no competing interests. **Data and materials availability:** All data needed to evaluate the conclusions in the paper are present in the paper and/or the Supplementary Materials.

Submitted 27 April 2023
Accepted 5 February 2024
Published 12 July 2024
10.1126/sciadv.adi4746